UDC 551.510.534:551.521.3:541.14

Effect of Photochemical Models on Calculated Equilibria and Cooling Rates in the Stratosphere

DONNA BLAKE—*The Florida State University, Tallahassee, Fla.*
RICHARD S. LINDZEN[1]—*Harvard University, Cambridge, Mass.*

ABSTRACT—Simplified models are developed for radiative heating and cooling and for ozone photochemistry in the region 22–61 km. The latter permit the inclusion of nitrogen and hydrogen reactions in addition to simple oxygen reactions. The simplicity of the scheme facilitates the use of a wide variety of cooling and reaction rates. We also consider determination of temperature and composition as a joint process. It is shown that joint radiative-photochemical equilibrium is appropriate to the mean state of the atmosphere between 35 and 60 km. Equilibrium calculations are then used to show that hydrogen reactions are important for ozone and temperature distributions primarily above 40 km while nitrogen reactions are important primarily below 50 km. Comparisons with observed distributions of temperature and ozone suggest the need for water vapor mixing ratios of from $1–5\times10^{-6}$ and mixing ratios of (NO_2+NO) of from $3–10\times10^{-8}$ at the stratopause. At 35 km, a mixing ratio of (NO_2+NO) of about 3×10^{-8} is indicated. The precise values depend on our choice of reaction and radiative cooling rate coefficients, and the simple formulation permits the reader to check the effect of new rates as they become available.

The relaxation of perturbations from joint radiative-photochemical equilibrium is also investigated. In all cases, the coupling between temperature-dependent ozone photochemistry and radiation lead to a reduction of the thermal relaxation time from its purely radiative value. The latter, which amounts to about 10 days at 35 km and decreases to about 5 days at 50 km, is reduced to 3–7 days at 35 km and to 1.5–2.5 days at 50 km. This greatly enhances the dissipation of waves traveling through the stratosphere.

1. INTRODUCTION

The equilibrium temperature in the stratosphere is determined by the approximate balance between heating due to absorption of solar ultraviolet energy by ozone and cooling due to infrared emission by the 15-μm band of carbon dioxide. [A certain amount of cooling also is due to O_3 9.6 μm emission, but this cooling is considerably less than that due to the 15-μm band of CO_2 (Murgatroyd and Goody 1958).] The rate of energy absorption and, therefore, the temperature depend on the ozone density.

Production of ozone is by the reaction

$$O+O_2+M\rightarrow O_3+M, \qquad (1)$$

which is markedly temperature dependent. This coupling between temperature and ozone density indicates that the relaxation time of a temperature perturbation should not be that due to carbon dioxide cooling alone but should be that due to carbon dioxide cooling modified by the effects of photochemistry.

Lindzen and Goody (1965) have calculated the thermal relaxation time for carbon dioxide cooling coupled with photochemical effects for a pure oxygen atmosphere. Since these calculations were made, the rate constants for pure oxygen reactions have been questioned, and alternative ones have been proposed. In addition, it now seems that reactions involving nitrogen and hydrogen compounds may be significant in determining the ozone distribution in the stratosphere (Hunt 1966, Leovy 1969*a*, Crutzen 1971); and such reactions, therefore, should be included in the photochemical model. Most of the rates for reactions involving hydrogen compounds are not temperature dependent; there is, therefore, a question as to the influence of these reactions on the coupling between ozone density and temperature. It has been suggested (Leovy 1969) that, if the hydrogen reactions are dominant in determining the ozone density, the appropriate thermal relaxation time is just that due to cooling from the 15-μm carbon dioxide band. As we shall show, this is untrue since relation (1) (i.e., the reaction $O+O_2+M\rightarrow O_3+M$) remains important in all schemes.

Cooling due to infrared emission by carbon dioxide and modified by photochemistry acts as damping on motions in the stratosphere. The time scale for this damping, which may be represented as Newtonian cooling, is simply the thermal relaxation time scale. As Dickinson (1969) shows, internal Rossby waves (excited in the troposphere) could carry large amounts of energy up to the lower thermosphere unless this time is much less than 10 days, 5–10 days being the approximate time scale for unmodified CO_2 15 μm cooling. Thus, the effects of photochemistry on this time scale could be crucial.

In this paper, we shall investigate the effect of photochemistry on the cooling rate for the height range 22–61 km. A simplified photochemical model that is suitable for this height range and that includes reactions involving nitrogen and hydrogen compounds is developed in section 2. The temperature equation for this photochemical

[1] Alfred P. Sloan Foundation Fellow

model is obtained in section 3. Vertical distributions of constituents and temperature for radiative-photochemical equilibrium are discussed in section 4. Linearized equations for the photochemistry and temperature are found in section 5 as are the relevant time scales for photochemical and thermal relaxation. Conclusions are presented in section 6.

Many reaction rate constants are uncertain by as much as an order of magnitude, so a wide range of values is used. Because mixing ratios for water vapor and nitrogen oxides are uncertain, several distributions are used. For the range of rates and ratios used, we found that including photochemistry reduces the thermal relaxation time scale above 35 km from the value appropriate when only infrared emission by carbon dioxide is considered. Furthermore, the minimum value for the thermal relaxation time scale nearly always occurs at a height between 45 and 50 km, with a secondary minimum at a height between 28 and 40 km. Finally, the minimum value for the thermal relaxation time scale is always 1/3 to 1/2 of that found at the same height when the photochemistry is ignored.

We also found that equilibrium distributions of temperature and ozone density vary with the different rate constants and ratios assumed. At the stratopause, relaxation time scales are short enough (approx. 90 min for ozone and a few days for temperature) that the equilibrium temperature should be close to the observed temperature of approximately 270°K (Valley 1965, Theon and Smith 1971). We attempt to match the observed temperature rather than the observed ozone densities, since the former is better determined than the latter between 35 and 61 km.

Our results show that neglecting nitrogen and hydrogen reactions leads to the prediction of excessive temperatures between 35 and 61 km. The prediction of observed temperatures between 50 and 61 km calls for water vapor mixing ratios of from $1–5\times10^{-6}$ depending on the reaction rate constants used. A mixing ratio for total nitrogen oxides ($NO+NO_2$) of 3×10^{-8} produces correct temperatures from 35 to 50 km. All such estimates depend on our choice of reaction and cooling rate coefficients, but the dependence has been specified in a simple manner.

2. PHOTOCHEMICAL MODEL

As many as 80 different reactions have been considered for an atmosphere consisting of nitrogen, hydrogen, oxygen, and their compounds (Hunt 1966, Shimazaki and Laird 1970, Crutzen 1971). For many problems, the full set of reactions may not be needed, and a much shorter set can be used for the photochemical model. It should be apparent that the simplified photochemical model developed in this section may not be the most suitable one for all problems.

For the current problem, we are interested primarily in the vertical distribution of ozone, the reactions that determine this distribution, and the temperature dependence of such reactions for the height range 22–61 km. Many reactions are important in only limited height ranges. Reactions that are important only above 61 km or below 22 km are not retained. The list of reactions retained is in table 1.

For each constituent found in table 1, it is possible to write a continuity relation

$$\frac{dn_i}{dt}+n_i\nabla\cdot\mathbf{V}=S_i-L_i \tag{2}$$

where d/dt is the substantive derivative $\partial/\partial t+\mathbf{V}\cdot\nabla$, $\mathbf{V}$ is the velocity vector, and n_i, S_i, and L_i are the number density, source term, and loss term, respectively, of the constituent i

$$[i=O(O(^3P)),O^*(O(^1D)),HO_2,\ OH,\ H,\ H_2O,\ H_2O_2,\ HNO_3,\ HNO_2,\ NO,\ NO_2,\ \text{and}\ NO_3].$$

Below 70 km,

$$\frac{n_i}{n_m}\ll1 \tag{3}$$

where n_m is the molecular number density; therefore, the continuity equation for n_m becomes

$$\frac{d}{dt}n_m+n_m\nabla\cdot\mathbf{V}=0. \tag{4}$$

Substituting eq (4) into eq (2) yields

$$\frac{d\left(\frac{n_i}{n_m}\right)}{dt}=\frac{S_i-L_i}{n_m}. \tag{5}$$

The ratio n_i/n_m for a constituent i is referred to as its mixing ratio.

The photochemical model now consists of 13 continuity equations of the form of eq (5). There are several relations among the constituents that will further simplify the model. Some of these relations have been pointed out previously (Dütsch 1968, Leovy 1969, Crutzen 1971).

Since below 61 km less than 1 percent of the H_2O molecules are dissociated in a day by reactions 3 and 8 (table 1), the mixing ratio of water vapor at a given height may be considered constant. Also, the adjustment time for equilibrium of O* is

$$t(O^*)=(k_7n_m)^{-1}<10^{-5}\text{s}$$

and that for H is

$$t(H)=(n_{O_2}n_mk_{10})^{-1}<4\text{s}.$$

Both of these constituents may be considered in equilibrium with concentrations

$$n_{O*}\approx\frac{q_{3b}n_{O_3}}{k_7n_m} \tag{6}$$

and

$$n_H\approx\frac{n_{OH}n_Ok_9}{n_{O_2}n_mk_{10}+n_{O_3}k_{27}}. \tag{7}$$

TABLE 1.—*Reaction rates that determine the vertical distribution of ozone as used in the photochemical model developed and described in this paper*

	Reaction	Rate	Source
1	$O_2+h\nu\rightarrow O+O$	$q_2(\lambda<2460$ Å)	See text.
2a	$O_3+h\nu\rightarrow O+O_2$	$q_{3a}(3100$ Å$<\lambda<11000$ Å)	See text.
2b	$O_3+h\nu\rightarrow O^*+O_2$	$q_{3b}(\lambda<3100$ Å)	See text.
3	$H_2O+h\nu\rightarrow H+OH$	$q_{H_2O}(\lambda<2400$ Å)	See text.
4	$NO_2+h\nu\rightarrow NO+O$	$q_{NO_2}(\lambda<3975$ Å)	See text.
5	$O+O_2+M\rightarrow O_3+M$	k_5	See table 2.
6	$O+O_3\rightarrow 2O_2$	k_6	See table 2.
7	$O^*+M\rightarrow O+M$	$k_7=5\times10^{-11}$	Zipf (1969)
8	$O^*+H_2O\rightarrow 2OH$	$k_8=3\times10^{-10}$	Paraskevopoulos and Cvetanovic (1971)
9	$OH+O\rightarrow H+O_2$	$k_9=5\times10^{-11}$	Kaufman (1969)
10	$H+O_2+M\rightarrow HO_2+M$	$k_{10}=4\times10^{-32}$	Kaufman (1969)
11	$HO_2+O\rightarrow OH+O_2$	$k_{11}=5\times10^{-11}$	Nicolet (1970)
12	$OH+O_3\rightarrow HO_2+O_2$	$k_{12}=1.3\times10^{-12}\exp(-950/T)$	Anderson and Kaufman (1973)
13	$OH+OH\rightarrow H_2O+O$	$k_{13}=1.38\times10^{-11}\exp(-500/T)$	Schofield (1967)
14	$OH+HO_2\rightarrow H_2O+O_2$	$k_{14}=2\times10^{-10}$	Hochanadel et al. (1972)
15	$HO_2+NO\rightarrow OH+NO_2$	$k_{15}=3\times10^{-12}T^{1/2}\exp(-1250/T)$	Nicolet (1970)
16	$NO_2+O\rightarrow NO+O_2$	$k_{16}=9.1\times10^{-12}$	Davis et al. (1973)
17	$NO+O_3\rightarrow NO_2+O_2$	$k_{17}=9.0\times10^{-13}\exp(-1200/T)$	Herron and Huie (1972)
18	$NO_2+O_3\rightarrow NO_3+O_2$	$k_{18}=10^{-11}\exp(-3500/T)$	Johnston and Yost (1949)
19	$NO_2+OH+M\rightarrow HNO_3+M$	$k_{19}=1.12\times10^{-31}\exp(900/T)$	Anderson, Margitan, and Kaufman (1973)
20	$NO+OH+M\rightarrow HNO_2+M$	$k_{20}=k_{19}$	See text.
21	$HNO_3+O\rightarrow NO_3+OH$	$k_{21}<10^{-14}$	Morris and Niki (1971)
22	$HNO_2+O\rightarrow OH+NO_2$	$k_{22}=k_{21}$	See text.
23	$NO_3+NO\rightarrow 2NO_2$	$k_{23}=10^{-11}$	Berces and Forgeteg (1970)
24	$HO_2+HO_2\rightarrow H_2O_2+O_2$	$k_{24}=3.3\times10^{-12}$	Foner and Hudson (1962) Paukert and Johnson (1972)
25	$H_2O_2+h\nu\rightarrow 2OH$	$q_{H_2O_2}(\lambda<5650$ Å)	Holt et al. (1948)
26	$H_2O_2+OH\rightarrow H_2O+HO_2$	$k_{26}=4\times10^{-13}T^{1/2}\exp(-600/T)$	Greiner (1968)
27	$H+O_3\rightarrow OH+O_2$	$k_{27}=1.5\times10^{-12}T^{1/2}$	Phillips and Schiff (1962)
28	$HNO_3+h\nu\rightarrow OH+NO_2$	$q_{HNO_3}(\lambda<6000$ Å)	Schmidt et al. (1972)
29	$HNO_2+h\nu\rightarrow OH+NO$	q_{HNO_2}	See text.

TABLE 2.—*Reaction rates used for the pure oxygen reactions (5 and 6) in table 1*

Set 1:
$k_5=1.2\times10^{-35}\exp(1000/T)$
$k_6=2.0\times10^{-11}\exp(-2395/T)$ } Schiff (1969)

Set 2:
$k_5=8.0\times10^{-35}\exp(445/T)$
$k_6=5.6\times10^{-11}\exp(-2850/T)$ } Benson and Axworthy (1965)

Set 3:
$k_5=1.0\times10^{-34}\exp(510/T)$ Huie et al. (1972)
$k_6=2.0\times10^{-11}\exp(-2410/T)$ Garvin (1972)

As Leovy (1969) indicates, eq (7) means that, when reaction 27 is small compared to reaction 10, the atomic hydrogen produced in reaction 9 is destroyed so rapidly by reaction 10 that the two reactions may be replaced by the single reaction

$$OH+O\rightarrow HO_2 \tag{8}$$

with the reaction rate k_9. This approximation is valid below 40 km; but at 40 km, about 10 percent of the ozone destruction *due to hydrogen reactions* is by reaction 27. Above this height, reaction 27 becomes increasingly important, accounting for about 20 percent of the total ozone destruction at 61 km. Thus, if reaction rates are significantly altered, reaction 27 could become a major one.

When the reactions involving O and O_3 are considered, it is apparent that the dominant reactions involve interconversion between O and O_3. The ratio

$$R_1=\frac{n_O}{n_{O_3}}\approx\frac{q_{3a}+q_{3b}}{n_{O_2}n_m k_5} \tag{9}$$

has an adjustment time,

$$t(R_1)=(q_{3a}+q_{3b}+n_{O_2}n_m k_5)^{-1}<10^2 \text{ s},$$

which is short compared to other time scales of interest; therefore, eq (9) remains valid. Similarly, the reactions involving interconversion between HO_2 and OH are dominant among those involving these two constituents. Below 40 km, where relation (8) (i.e., the reaction $OH+O\rightarrow HO_2$) may be used,

$$R_2=\frac{n_{HO_2}}{n_{OH}}\approx\frac{n_O k_9+n_{O_3}k_{12}}{n_O k_{11}+n_{NO}k_{15}}, \tag{10}$$

which has an adjustment time of

$$t(R_2)=(n_O k_9+n_{O_3}k_{12}+n_O k_{11}+n_{NO}k_{15})^{-1}<100 \text{ s}.$$

Above 40 km,

$$n_{OH}\approx\frac{n_{HO_2}n_O k_{11}+n_H n_{O_3}k_{27}}{n_O k_9} \tag{11}$$

and

$$n_{HO_2} \approx \frac{n_H n_{O_2} n_m k_{10} + n_{OH} n_{O_3} k_{12}}{n_O k_{11}}, \quad (12)$$

which have adjustment times

$$t(OH) = (n_O k_9)^{-1} < 15 \text{ s}$$

and

$$t(HO_2) = (n_O k_{11})^{-1} < 15 \text{ s}.$$

Therefore, when eq (7) is used in eq (12), the resulting ratio is

$$R_2 = \frac{n_{HO_2}}{n_{OH}} \approx \frac{k_9}{k_{11}} \left(1 + \frac{n_{O_3} k_{27}}{n_{O_2} n_m k_{10}}\right)^{-1} + \frac{k_{12}}{R_1 k_{11}}. \quad (13)$$

The term $k_{12}/R_1 k_{11}$ in eq (13) becomes negligibly small above 45 km. Finally, by similar arguments, one gets a ratio,

$$R_3 = \frac{n_{NO}}{n_{NO_2}} \approx \frac{n_O k_{16} + q_{NO_2}}{n_{O_3} k_{17}}, \quad (14)$$

which has an adjustment time

$$t(R_3) = (n_O k_{16} + q_{NO_2} + n_{O_3} k_{17})^{-1} < 200 \text{ s}.$$

The three constituents, HNO_3, HNO_2, and NO_3, are approximately in equilibrium with values of

$$n_{HNO_3} \approx \frac{k_{19} n_m n_{NO_2} n_{OH}}{k_{21} n_O + q_{HNO_3}}, \quad (15)$$

$$n_{HNO_2} \approx \frac{k_{20} n_m n_{OH} n_{NO}}{k_{22} n_O + q_{HNO_2}}, \quad (16)$$

and

$$n_{NO_3} \approx \frac{k_{21} n_O n_{HNO_3} + k_{18} n_{NO_2} n_{O_3}}{k_{23} n_{NO}}. \quad (17)$$

Their adjustment times are:

$$t(HNO_3) = (k_{21} n_O + q_{HNO3})^{-1} < 10^3 \text{ s},$$

$$(HNO_3) < 10^5 - 10^6 \text{ s (below 35 km)},$$

and

$$t(NO_3) = (k_{23} n_{NO})^{-1} < 2 \times 10^3 \text{ s}.$$

These times may be sufficiently long for the use of equilibrium values to be questioned.

The longer time scales for HNO_3 are based on HNO_3 absorption measurements by Dalmon (reported by Schmidt et al. 1972) while the shorter time scales are based on measurements by Schmidt et al. (1972). If the smaller time scales apply, then the densities of HNO_3 and HNO_2 estimated by eq (15) and (16) are small enough relative to the densities of NO, NO_2, OH, and HO_2 to indicate that HNO_3 and HNO_2 are of minor importance in determining the vertical distribution of O_3. Similarly, the NO_3 density estimated by eq (17) is small enough to be neglected in determining the vertical distribution of O_3. On the other hand, if the actual time scales for HNO_3 and HNO_2 are closer to the larger values indicated, then (below 35 km) the available NO and NO_2 are gradually converted to HNO_3 and HNO_2. Since reactions involving NO and NO_2 (reactions 16 and 17) are much more important to the ozone distribution than those involving HNO_2 and HNO_3 (reactions 21 and 22), this conversion means the odd nitrogen is gradually converted below 35 km to forms that do not affect the ozone distribution significantly. Then HNO_3 and HNO_2 diffuse upward and downward from the lower stratosphere where they are formed. Since the photodissociation rate of HNO_3 increases with height, the HNO_3 that diffuses upward will eventually be dissociated, thereby increasing the NO_x and affecting the ozone distribution at the height where dissociation occurs. The effect of the approximations found in eq (15), (16), and (17) are discussed further in section 4.

The total odd nitrogen density is the sum of the densities of NO, NO_2, NO_3, HNO_2, and HNO_3. Since the list of reactions in table 1 does not contain sources or losses for the total odd nitrogen density, the continuity equation is

$$\frac{d}{dt} \frac{(n_{NO} + n_{NO2} + n_{NO_3} + n_{HNO_3} + n_{HNO_2})}{n_m} = 0; \quad (18)$$

or using eq (15), (16), and (17) in eq (18), one obtains

$$\frac{d}{dt} \frac{(n_{NO} + n_{NO_2})}{n_m} = 0. \quad (19)$$

Two sources of total odd nitrogen in the region 22–61 km are considered to be downward diffusion of NO from above 70 km where it is formed and the upward diffusion of N_2O from the troposphere, which is then destroyed by the reaction

$$N_2O + O^* \rightarrow 2NO \quad (20)$$

with a rate $k = 9 \times 10^{-11}$ cm^3/s (Donovan and Husain 1970). The mixing ratio of N_2O is 2.5×10^{-7} at the tropopause and apparently decreases with height (Schütz et al. 1970). If we estimate the mixing ratio of $NO + NO_2$ as 10^{-9}–10^{-7} (Junge 1963, Barth 1966, Pearce 1969), then the time scale for an increase in odd nitrogen density due to the two sources described is estimated to be several weeks. The possible losses to the odd nitrogen density are downward diffusion of the constitutents or conversion to N_2O_5 followed by downward diffusion of that constituent.

Rather than try to include the source and loss terms for the odd nitrogen concentration, we have decided to use eq (18) or, equivalently, to set

$$\frac{n_{NO} + n_{NO_2}}{n_m} = K \quad (21)$$

where K is a mixing ratio that is constant in time but a possible function of height. This highly simplified treatment of the nitrogen constituents may be justified on the grounds that *we are not seeking a detailed time and height distribution for each nitrogen constituent but are trying to evaluate the importance of the nitrogen reactions to the distribution of ozone.* A more detailed study of the dis-

tribution of odd nitrogen compounds may be found in McConnell and McElroy (1973).

The constituent H_2O_2 is produced in reaction 24 and destroyed in reactions 25 and 26. The net result is the loss of HO_2 back into H_2O. This conversion also occurs in reaction 14. If reactions 24, 25, and 26 are neglected, the result is that the calculated sum, $n_{OH}+n_{HO_2}$, is too large. However, the change in the sum $n_{OH}+n_{HO_2}$, occurring when these reactions are ignored, is significant only below 35 km. We will show in sections 4 and 5 that the reactions involving hydrogen are significant only above 40 km. Therefore, reactions 24, 25, and 26 are to be neglected.

The constituents O*, H, HNO_3, HNO_2, and NO_3 are considered to be in equilibrium [eq (6), (7), (15), (16), and (17)]; and the water vapor mixing ratio is considered constant in time while H_2O_2 is neglected. Therefore, the continuity relations [eq (5)] are needed for only the six consitituents, O, O_3, NO, NO_2, HO, and HO_2. By using eq (9), (10), and (14), we reduce the six continuity relations to three:

$$\frac{d}{dt}(1+R_1)\phi=C-A\phi^2-B\phi\psi-FX\phi, \tag{22}$$

$$\frac{d}{dt}(1+R_2)\psi=D\phi+G-E\psi^2, \tag{23}$$

and

$$\frac{d}{dt}(1+R_3)X=0 \tag{24}$$

where

$$\phi\equiv\frac{n_{O_3}}{n_m},$$

$$\psi\equiv\frac{n_{OH}}{n_m},$$

and

$$X\equiv\frac{n_{NO_2}}{n_m}$$

with

$$C=2q_2\frac{n_{O_2}}{n_m}, \tag{25}$$

$$A=2R_1k_8n_m, \tag{26}$$

$$B=(R_1k_9+R_1R_2k_{11}+k_{12})n_m \qquad z\leq 40\text{ km}, \tag{27}$$

$$B=\left[R_1k_9+R_1R_2k_{11}+R_1k_9\left(1+\frac{n_{O_2}n_mk_{10}}{n_{O_3}k_{27}}\right)^{-1}+k_{12}\right]n_m \qquad z\geq 40\text{ km}, \tag{28}$$

$$F=(2R_1k_{16}+k_{18})n_m, \tag{29}$$

$$D=\frac{2k_8n_{H_2O}q_{3b}}{k_7n_m}, \tag{30}$$

$$G=\frac{2q_{H_2O}n_{H_2O}}{n_m}, \tag{31}$$

and

$$E=2(k_{13}+R_2k_{14})n_m. \tag{32}$$

Using eq (13) in eq (28), we get

$$B\approx 2(R_1k_9+k_{12})n_m. \tag{33}$$

Had we formally retained eq (27) above 40 km, then we would also obtain eq (33) as an approximation. Thus eq (27) may be used at all heights with only small errors. As with eq (13), k_{12} in eq (33) may be neglected above 45 km.

Equations (6), (7), (9)–(17), and (22)–(32) together with the reaction rates in table 1 comprise the photochemical model to be used in sections 3, 4, and 5.

3. ENERGY RELATION

The energy relation is

$$\rho c_v\frac{dT}{dt}=S+p\nabla\cdot\mathbf{V} \tag{34}$$

where p is pressure, T is temperature, ρ is density, and c_v is the heat capacity at constant volume. Here,

$$S\equiv\hat{E}+C \tag{35}$$

where $\hat{E}$ represents energy absorbed and C is the heat exchange due to infrared radiation. In the atmosphere, the fractional pressure change is small for velocities less than that of sound (Jefferys 1930). This permits eq (34) to be approximated by

$$\frac{dT}{dt}+w\frac{g}{c_p}=\frac{1}{\rho c_p}(\hat{E}+C) \tag{36}$$

where c_p is the heat capacity at constant pressure, g is the gravitational constant, and w is the vertical velocity. [See Ogura and Phillips (1962) for an analysis of the validity of eq (36); Holton (1972) shows that eq (36) is rigorously correct in a coordinate system where log p replaces z.]

As discussed in the introduction, the major source of cooling in the region 22–61 km is the 15-μm band of carbon dioxide. This cooling is proportional to the local blackbody function (Rodgers and Walshaw 1966), which (for the range of temperatures found in the stratosphere) can be approximated as a linear function of temperature. Thus, the cooling or thermal emission is

$$\frac{1}{\rho c_p}C\approx -aT+b \tag{37}$$

where a is a function of height. We use two different distributions of a and b:

1. (Lindzen and Goody 1965)

$a=(17\text{ days})^{-1}$

and

$b=a\ (180)°\text{K}$

and

2. (Dickinson 1973)

$$a=(10\text{ days})^{-1}\left(1+\frac{z-35.8}{20.8}\right) \qquad z<35.8\text{ km},$$

$$a=(10\text{ days})^{-1}+(8.64\text{ days})^{-1}\left(\frac{z-35.8}{14.2}\right) \qquad 35.8\text{ km}\leq z<50\text{ km},$$

$$a=(4.63\text{ days})^{-1} \qquad 50\text{ km}\leq z<54.4\text{ km},$$

and

$$a=(4.63\text{ days})^{-1}-(26.3\text{ days})^{-1}\left(\frac{z-54.4}{6.4}\right) \qquad 54.4\text{ km}\leq z\leq 61\text{ km}$$

with

$$b=a[195+1.09(z-48)]^{\circ}\text{K} \qquad z\leq 48\text{ km}$$

and

$$b=a\left[187+\frac{(61-z)}{1.57}\right]^{\circ}\text{K} \qquad z\geq 48\text{ km}.$$

These two distributions, referred to as slow and fast infrared cooling, respectively, offer a range of cooling rates. They show the effect that changing the infrared cooling rate has on the stratospheric temperature and ozone distributions.

The energy source may be written as

$$\hat{E}=\sum_l r_l\epsilon_l \tag{38}$$

where r_l is the number of reactions per second per cubic centimeter for reaction l and ϵ_l is the energy gain per reaction. The ϵ_l consists of dissociation energy, D_l, and solar energy absorbed, E_l. With these definitions, eq (33) becomes

$$\hat{E}=\Sigma r_l(E_l+D_l). \tag{39}$$

Solar energy absorbed by O_3, O_2, H_2O, and NO_2 contributes to the source terms as:

$$\sum_l r_l E_l=\bar{h\nu}_{O_2}q_2n_{O_2}+\bar{h\nu}_{O_3}(q_{3a}+q_{3b})n_{O_3} +\bar{h\nu}_{NO_2}q_{NO_2}n_{NO_2}+\bar{h\nu}_{H_2O}q_{H_2O}n_{H_2O} \tag{40}$$

where

$$q_j(z)=\int a_j I_{0\nu}\exp\left(-\sum_j a_j x_j\right)d\nu \qquad j=O_2,\ O_3,\ HO_2,\ NO_2 \tag{41}$$

and

$$\bar{\nu}_j=q_j^{-1}\int a_j\nu I_{0\nu}\exp\left(-\sum_j a_j x_j\right)d\nu. \tag{42}$$

Here, $a_j(\nu)$ is the absorption cross section in square centimeters of the jth constituent, $I_{0\nu}$ is the photon flux incident at the top of the atmosphere, x_j is the total number of molecules per square centimeter of the jth constituent between the top of the atmosphere and the altitude z, h is the Planck constant, and $\bar{\nu}_j$ is the mean frequency of solar photons absorbed by the jth constituent. Representative variations of $(q_{3a}+q_{3b})n_{O_3}$, $q_2n_{O_2}$, $q_{H_2O}n_{H_2O}$, and $q_{NO_2}n_{NO_2}$ with height are shown in figure 1. It is apparent that

$$(q_{3a}+q_{3b})n_{O_3}\gg q_2n_{O_2}$$

and

$$(q_{3a}+q_{3b})n_{O_3}\gg q_{H_2O}n_{H_2O}$$

at all heights. Since $\bar{h\nu}_{O_3}/\bar{h\nu}_{O_2}$ and $\bar{h\nu}_{O_3}/\bar{h\nu}_{H_2O}$ vary between 1 and 1/3, the term $\bar{h\nu}_{O_3}(q_{3a}+q_{3b})n_{O_3}$ is much larger than $\bar{h\nu}_{H_2O}q_{H_2O}n_{H_2O}$ or $\bar{h\nu}_{O_2}q_2n_{O_2}$ at all heights. The latter two terms, therefore, may be neglected in eq (40). Above 30 km,

$$\bar{h\nu}_{O_3}(q_{3a}+q_{3b})n_{O_3}\gg\bar{h\nu}_{NO_2}q_{NO_2}n_{NO_2}.$$

Below 30 km, the ratio

$$\frac{(q_{3a}+q_{3b})n_{O_3}}{q_{NO_2}n_{NO_2}}\geq 8,$$

provided the mixing ratio of NO_2 does not exceed 3×10^{-8} (the value used in calculating $q_{NO_2}n_{NO_2}$ for fig. 1). Since

$$\frac{\bar{h\nu}_{O_3}}{\bar{h\nu}_{NO_2}}\approx 0.7$$

below 30 km, the term

$$\bar{h\nu}_{O_3}(q_{3a}+q_{3b})n_{O_3}>\bar{h\nu}_{NO_2}q_{NO_2}n_{NO_2}$$

at all heights, and the latter term is neglected in eq (40). Then eq (40) becomes

$$\sum_l r_l E_l\approx\bar{h\nu}_{O_3}(q_{3a}+q_{3b})n_m\phi. \tag{43}$$

The second part of the energy source term in eq (39) can be written as

$$\begin{aligned}\sum_l r_l D_l=&D(O_3)n_m\frac{d}{dt}\left(\frac{n_{O_3}}{n_m}\right)-\frac{1}{2}D(O_2)n_m\left[\frac{d}{dt}\left(\frac{n_O}{n_m}\right)+\frac{d}{dt}\left(\frac{n_{O_3}}{n_m}\right)\right]\\&+D(HO_2)n_m\frac{d}{dt}\left(\frac{n_{HO_2}}{n_m}\right)\\&+\frac{1}{2}D(OH)n_m\left[\frac{d}{dt}\left(\frac{n_{OH}}{n_m}\right)-\frac{d}{dt}\left(\frac{n_{HO_2}}{n_m}\right)\right]\\&-\frac{1}{2}D(H_2O)n_m\left[\frac{d}{dt}\left(\frac{n_{HO_2}}{n_m}\right)+\frac{d}{dt}\left(\frac{n_{OH}}{n_m}\right)\right]\\&+D(NO_2)n_m\frac{d}{dt}\left(\frac{n_{NO_2}}{n_m}\right)\end{aligned} \tag{44}$$

where $D(j)$ is the dissociation energy of the jth constituent. We have evaluated eq (44) in detail and have found that its contribution is always small. We will spare the reader the specifics. (Note that eq (44) is identically zero for equilibrium.)

Thus eq (34) becomes

$$\frac{dT}{dt}+w\frac{g}{c_p}=\eta\phi-aT+b \tag{45}$$

where

$$\eta=\bar{h\nu}_{O_3}(q_{3a}+q_{3b})\frac{n_m}{\rho c_p}. \tag{46}$$

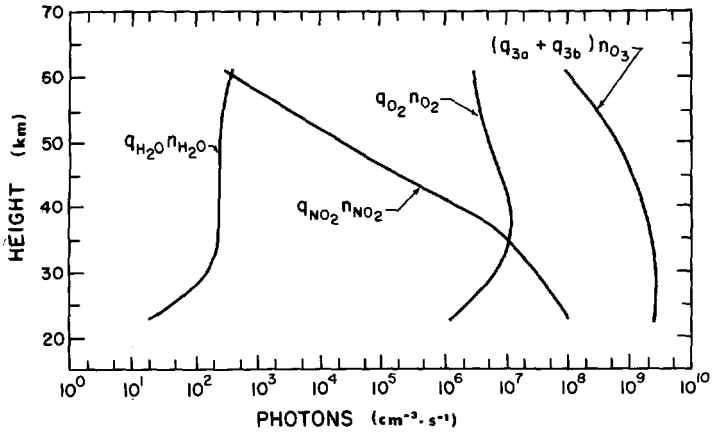

FIGURE 1.—Absorption of solar photons by NO_2, O_2, H_2O, and O_3 as a function of height.

It is apparent from eq (45) and (46) that the equilibrium temperature is determined by the approximate balance between absorption of solar ultraviolet energy by ozone, $\eta\phi$, and cooling due to infrared emission by the 15-μm band of carbon dioxide, $-aT+b$.

4. RADIATIVE-PHOTOCHEMICAL EQUILIBRIUM

The photodissociation rates and energy absorption all vary with the solar zenith angle; thus local changes in temperature and composition have a time scale of 1 day. The photochemical relaxation time scales are less than 1 day above 35 km for all constituents, so calculations made with the local time changes in composition neglected should still give realistic distributions of constituents. However, the thermal relaxation time scale is a minimum of 2–3 days (see sec. 5). An estimate of the daily variation in temperature due to changing zenith angle of the sun can be made. The maximum energy absorption per day is at 50 km; therefore, the maximum daily variation in temperature would be expected at this height. At 50 km, the energy absorption rate at noon is about 3×10^{-10} J·cm^{-3}·s^{-1}. Roughly one-half of this energy goes to maintain the mean temperature. The noontime flux is also about half the amplitude of the diurnal oscillation in absorption. Then, from eq (45), the daily variation in temperature is estimated by

$$\frac{\partial(T)_d}{\partial t}\approx(\eta\phi)_d-a(T)_d \tag{47}$$

where the subscript d refers to the daily variation and $a=(10\text{ days})^{-1}$, $\rho=10^{-6}$ g·cm^{-3}, and $c_p=1$J·g^{-1}·°K^{-1}. Thus $(T)_d\approx2$°K, which is small enough that calculations made with the local temperature change neglected should still give realistic estimates of the temperature.

In the temperature relation [eq (45)], the advective terms are

$$u\frac{\partial T}{\partial x}+v\frac{\partial T}{\partial y}+w\left(\frac{\partial T}{\partial z}+\frac{g}{c_p}\right). \tag{48}$$

The size of the winds and temperature gradients can be estimated from Leovy (1964*a*, 1964*b*) who calculated thermally driven circulations in the stratosphere and mesosphere. Between 35 and 61 km, the mean advective terms are at least an order of magnitude less than the remaining terms. For example, at 50 km, $\partial T/\partial y\approx3\times10^{-3}$ °K/km, $dT/dz\approx0$, $v\approx0.6$ m/s, $w\approx0.08$ cm/s, and $g/c_p=10$°K/km; therefore, the vertical advective term is approximately 8×10^{-6} °K/s, and the horizontal advective term is approximately 2×10^{-6} °K/s. Since the cooling term $aT-b$ is approximately 10^{-4} °K/s, the advective terms can be neglected in the temperature equation. Similarly, the advective terms in the continuity equations can be neglected. For example, at 50 km, the vertical scale for the ozone mixing ratio is about 24 km; therefore, the time scale for change due to advection is approximately 3×10^{7} s. At 50 km, the ozone relaxation time is 5.4×10^{3} s; thus the advective terms can be neglected. Below 30 km, however, the ozone relaxation time scale increases rapidly to 3×10^{7} s while the advective time scale decreases. Therefore, below 30 km, the advective terms are important in determining the ozone distribution in the atmosphere.

Eddy transport of heat, as well as that due to the mean circulation, must be considered. Murgatroyd (1970) has calculated representative values of transient and standing eddy fluxes at several latitudes and heights (up to about 24 km) for the solstices. From his values, we estimate the vertical and horizontal eddy transport terms to be less than 10^{-6}°K/s in the summer hemisphere and equatorward of 40° in the winter hemisphere. Above 24 km, estimates of the eddy heat transport terms are scarce. Murgatroyd (1970) gives standard deviations of temperature and zonal velocities from their mean values for heights up to 60 km. From these values, a rough estimate of

$$\frac{\partial\overline{v'T'}}{\partial y}<2\times10^{-5}\text{ °K/s}$$

can be made for all latitudes in the summer hemisphere and equatorward of 30° in the winter hemisphere. The standard deviation of the vertical velocity is not given; but if it is not more than a few centimeters per second, then use of the scale height as the vertical scale yields

$$\frac{\partial\overline{w'T'}}{\partial z}<10^{-5}\text{ °K/s}$$

at all latitudes in the summer hemisphere and equatorward of 50° in the winter hemisphere. These estimates of the eddy transport of heat are crude, but they indicate that, away from the polar regions, these eddy transport terms can be neglected when compared to the cooling term $aT-b\sim10^{-4}$ °K/s [especially if one only wants a gross estimate of the temperature (within 10°K or so)].

The possibility also exists that the tides excited by solar heating could produce mean fluxes of importance to the mean thermodynamic budget. Careful checks, using the the results of Lindzen and Blake (1971), indicate that this is not the case below 90 km. Thus radiative-photochemical equilibrium seems appropriate from 35 to 61 km.

For radiative-photochemical equilibrium, eq (22), (23), and (45) become

$$0=C-A\phi^2-B\phi\psi-FX\phi, \tag{49}$$

$$0=D\phi+G-E\psi^2, \tag{50}$$

and

$$0=-aT+b+\eta\phi. \tag{51}$$

The distribution of ϕ, ψ, and T with height for equilibrium is found by solving eq (49), (50), and (51) simultaneously. The solution depends on the mixing ratios of water vapor and the nitrogen oxides and on the values of the rates used for the reactions listed in table 1.

As indicated in the preceding paragraphs, these three equations are valid for the height range 35–61 km. Below this height, the photochemical and thermal relaxation time scales become long enough that the neglected terms, particularly the advective terms, should be retained to find temperature and ozone distributions that agree with those observed. For convenience, eq (49), (50), and (51) are used for the entire height range 22–61 km, with the stipulation that the resulting radiative-photochemical equilibrium distributions are not expected to agree with those observed below 35 km.

An equilibrium solution also depends on η, q_{3a}, q_{3b}, q_{H_2O}, and q_{NO_2}, which are calculated at each height using eq (41), (42), and (46). The spectral region 1755–3950 Å is divided into 38 frequency intervals, and the region 4750–7000 Å is divided into four intervals. Below 61 km, nearly all photodissociation of O_2, O_3, H_2O, and NO_2 is due to absorption of photons in these two spectral regions. Incident photon fluxes, $I_{0\nu}$, are obtained from Kondratyev (1969) for the spectral regions above 3100 Å and from Brinkmann et al. (1966) for the region below 3100 Å. Hinteregger (1970) suggested that the photon fluxes found in Brinkmann et al. (1966) for the spectral region below 1800 Å may be too large by as much as a factor of 3. Below 61 km, the absorption of photons with energies corresponding to wavelengths less than 1800 Å makes only a small contribution to dissociation rates of O_2, O_3, H_2, and NO_2 (since they have already been absorbed by O_2). Therefore, the question of the magnitude of photon fluxes for the spectral region below 1800 Å is not important for our calculations.

Actual cross sections, α_j, for absorption by the jth constituent vary with frequency. For each frequency interval, the average cross section, $\bar{\alpha}_j$, was used. Cross sections for O_3 are from Griggs (1968) and Inn and Tanaka (1953); those for H_2O are from Watanabe and Zelikoff (1953) and Thompson et al. (1963); and those for NO_2 are from Hall and Blacet (1952) and Nakayama et al. (1959). It is more difficult to determine the appropriate cross section for O_2 in a given frequency interval due to the presence of the Schumann-Runge absorption band, which has numerous narrow rotation lines. One way of treating the absorption in the Schumann-Runge band is to consider the absorption cross section for O_2 as a function of both frequency and path length (Hudson et al. 1969). Then it is possible to divide the atmosphere into vertical layers and calculate the absorption coefficient of a given frequency interval for each layer (Brinkmann 1969). The atmosphere between 61 and 22 km is divided into 24 layers.

The water vapor mixing ratio is not well determined in the stratosphere. Some observations (Mastenbrook 1968, Schölz et al. 1970) indicate values of 3×10^{-6}–5×10^{-6} at 29 km and 3×10^{-6}–10×10^{-6} at 50 km. The value of the mixing ratio used at a given height is important at lower heights only if water vapor is a significant absorber of solar photons or if the hydrogen reactions strongly affect the ozone density since ozone is a strong absorber of solar energy. In the height range 22–61 km, the attenuation of incoming solar radiation due to absorption by water vapor is negligible. Hydrogen reactions are dominant in determining the ozone density above 40 km for a water vapor mixing ratio of 5×10^{-6}. The height above which the hydrogen reactions are dominant increases with decreasing water vapor mixing ratio. Since attenuation of solar energy by ozone is small above 50 km, it is only at heights below this that the vertical distribution of water vapor above is important. The effect of varying the mixing ratio of water vapor with height is not investigated here. For convenience, the mixing ratio for water vapor is assumed to be constant with height and is varied from 0 to 10^{-8}, 10^{-7}, 10^{-6}, 1.5×10^{-6}, 5×10^{-6}, or 10^{-5} in our various runs, not all of which will be described. We will describe the most realistic results, leaving the effects of other values to discussion.

As indicated in section 2, the vertical distribution for the mixing ratio of the nitrogen oxides, NO and NO_2, is not well known. The mixing ratio of nitrogen oxides, K, is defined in eq (21) and may be written by use of eq (14) as

$$K=(1+R_3)X. \tag{52}$$

Since the vertical distribution for the mixing ratio of nitrogen oxides is uncertain, the expedient choice is made of setting K as constant with height. Again, while values of K ranging from 10^{-9} to 3×10^{-7} were used in our computations, only the most realistic results will be shown in detail.

Reaction rate coefficients (for reactions 5–26, table 1) are somewhat uncertain. Three different sets of rates are used for reactions 5 and 6 (the pure oxygen reactions); these three sets are listed in table 2. The rates for reactions 7–26 are individually increased or decreased by a factor of 10, and the equilibrium distributions of constituents and temperatures are recalculated. Note that the rates for reactions involving HNO_2 are not known. We assumed that these rates are the same as those for similar reactions involving HNO_3. This assumption is admittedly a guess, which permits an estimate of the number density of HNO_2. If the shorter equilibrium time scales $t(HNO_3)$ and $t(HNO_2)$ are used, then the equilibrium estimate of HNO_2 by eq (16) is adequate for the current work. If the equilibrium time scales for HNO_3 and HNO_2 are the larger values given in section 2, then the equilibrium distributions are not valid estimates. In that case, NO and NO_2 are gradually converted into HNO_2 and

HNO_3, which act as sinks for odd nitrogen. This conversion would be more important at lower altitudes in the stratosphere where destruction by photodissociation is less than that at higher altitudes. If HNO_3 and HNO_2 increase in the lower stratosphere, upward as well as downward diffusion can occur. As HNO_3 and HNO_2 diffuse upward, they will be dissociated and contribute to the NO_x at the height where the dissociation occurs. It should be noted that the equilibrium number density for HNO_3 estimated from eq (15) is closer to observed values (Murcray et al. 1969) when the longer time scales are used (i.e., smaller photodissociation rates).

In solving eq (49), (50), and (51), consideration must be given to the fact that the thermal emission, as represented in eq (51) by $-aT+b$, occurs 24 hr a day while the absorption of solar energy and the photochemistry, as given by the other terms in the three equations, occur only during the daylight hours. The average of these time dependent terms over 24 hr, therefore, is needed for the equilibrium calculations. Time dependent calculations, which will be reported elsewhere, indicate that a good approximation to the time-averaged value of time dependent terms for heights between 35 and 60 km can be found by dividing the noontime value of the terms by 2.5. Since absorption of solar energy at a given height is also a function of latitude, equilibrium calculations are made at two latitudes, 0° and 45°.

Figures 2 and 3 (0° latitude, equinox) and figures 4 and 5 (45° latitude, equinox) show the radiative-photochemical distributions of temperature and ozone number density for four cases: (1) O (hydrogen and nitrogen reactions neglected), (2) H+O (nitrogen reactions neglected), (3) N+O (hydrogen reactions neglected), and (4) N+H+O. For all four cases, the rates in set 3 (table 2) are used for reactions 5 and 6, and the fast vertical distributions are used for a and b. When the nitrogen reactions are included, the mixing ratio for nitrogen oxides is 3×10^{-8}; when the hydrogen reactions are included, the water vapor mixing ratio is 1.5×10^{-6}.

Differences among the four different cases are most striking in the temperature profile (figs. 2, 4). The O case shows a linear increase in temperature up to 45 km and then a very small change in temperature above. The inclusion of the nitrogen reactions decreases the equilibrium temperature and ozone density below 45 km and has little effect on the distributions above 45 km. The temperature below 45 km is considerably reduced (approx. 20° K) from the pure O case, and the ozone density below 40 km is also considerably reduced (approx. 40 percent at 40 km to a factor of 3 at 22 km).

Inclusion of the hydrogen reactions has little effect below 45 km; but above this height, it strongly reduces the ozone density and temperature from the values found for the pure O case. When the hydrogen reactions are included, they are dominant in determining the temperature and ozone density above 45 km even when the nitrogen reactions are also included. Most significantly, there appears to be no way of producing a temperature decrease of the observed magnitude above the stratopause without including hydrogen reactions.

Water vapor must be dissociated before the resultant constituents H, OH, and HO_2 can act by means of the hydrogen reactions to reduce ozone density and thus temperature. It might be expected, since the mixing ratio of water vapor is assumed constant with height, that the hydrogen reactions would be important at all heights, not just above 45 km. However, the dissociation of water vapor is strongly height dependent. The photodissociation of water vapor below 61 km is due to absorption of solar radiation with energies corresponding to wavelengths below 2000 Å, which are strongly attenuated below 85 km due to absorption by O_2 and O_3. As a result, q_{H_2O} decreases from $4.3\times10^{-8}s^{-1}$ at 61 km to $1.1\times10^{-11}s^{-1}$ at 22.5 km. Water vapor is also dissociated in reaction 8, and the rate of dissociation depends on the density of O*. According to eq (6), the density of O* is proportional to q_{3b}, which is the absorption rate of radiation by ozone below 3100 Å. The radiation below 3100 Å is significantly attenuated below 45 km, and q_{3b} decreases from $8\times10^{-3}s^{-1}$ at 45 km to $1.1\times10^{-4}s^{-1}$ at 22.5 km. The dissociation of water vapor, therefore, increases with height; and as a result, the hydrogen reactions are more important to equilibrium distribution of ozone density and temperature with increasing height.

Equilibrium temperature profiles are shown in figure 6 for the three different sets of rates for reactions 5 and 6 and for the two cooling rate coefficients, fast and slow. The mixing ratio used for water vapor is 1.5×10^{-6}, and the mixing ratio used for nitrogen oxides is 3×10^{-8}. The slow cooling rate coefficient ($a^{-1}=17$ days) is 3.5 times as long as the fast one ($a^{-1}=4.83$ days) at 50 km. From eq (51), one might expect that a decrease of 3.5 in a would lead to an increase of 3.5 in $(T-b/a)$ rather than the factor of 2 increase (at 50 km) indicated in figure 6. Such is not the case since the ozone density itself is strongly temperature dependent through reactions 5 and 6 and increasing the temperature decreases the ozone density and thus the absorption of energy. Therefore, the equilibrium temperature is *buffered* against change. An alteration in the cooling is partly compensated for by a corresponding alteration in the heating, so the fractional change in the equilibrium temperature is actually much smaller than the fractional changes in either the cooling or heating.

Coupling of temperature and ozone density is obvious for an O atmosphere (neglecting the hydrogen and nitrogen reactions) since eq (49) becomes

$$0=C-A\phi^2 \tag{53}$$

and, from eq (26) and (9),

$$A=\frac{2(q_{3a}+q_{3b})k_6}{n_{O_2}k_5}. \tag{54}$$

in which the ratio k_6/k_5 is strongly temperature dependent. Note that, for each set of rates for k_5 and k_6 in table 2, the ratio k_6/k_5 is strongly temperature dependent. In fact, the temperature dependence of k_6/k_5 for set 1 is

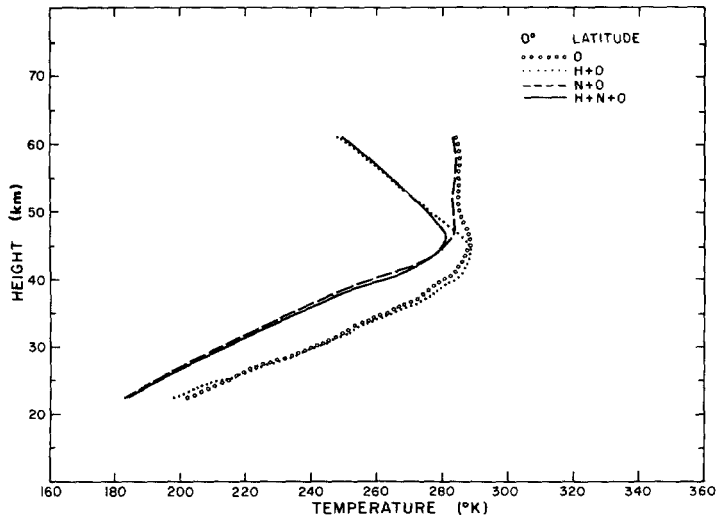

FIGURE 2.—Radiative-photochemical equilibrium temperature for 0° latitude at the equinox as a function of height.

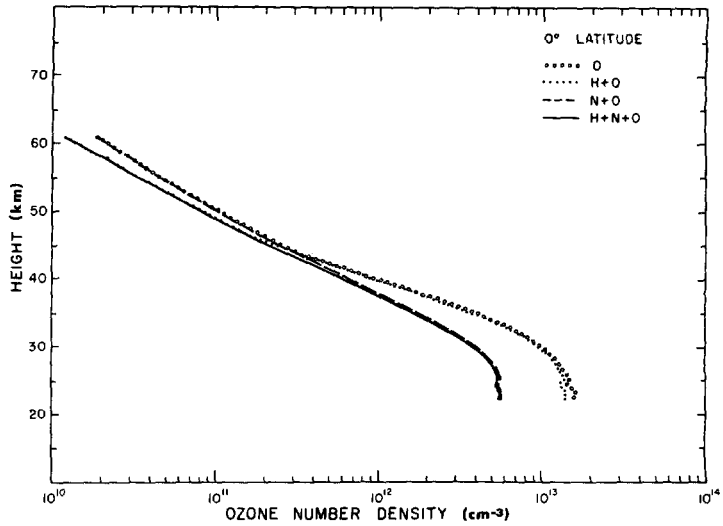

FIGURE 3.—Radiative-photochemical equilibrium ozone number density for 0° latitude at the equinox as a function of height.

$\exp(-3395/T)$, which is very close to that of $\exp(-3295/T)$ found for set 2. The temperature dependence of set 3 is somewhat less at $\exp(-2920/T)$. When hydrogen reactions are dominant in determining the ozone density (as appears to be the case above 45 km for a water vapor mixing ratio of 1.5×10^{-6}), it might appear that the temperature dependence of the ozone density would be greatly reduced since the hydrogen reactions do not have rates that are strongly temperature dependent. Above 45 km, eq (49) can be approximated, by use of eq (27) and (9), as

$$0=C-B\phi\psi \tag{55}$$

where (above 45 km)

$$B\approx\frac{2(q_{3a}+q_{3b})k_9}{n_{O_2}k_5}. \tag{56}$$

[Note that $-A\phi^2$ still makes a sizable contribution to the destruction of ozone up to 52 km; but this form, eq (56), is used to illustrate the specific effects of the hydrogen reactions.] It is true that k_9 is not temperature dependent, but k_5 is strongly temperature dependent. Therefore, the presence of hydrogen reactions does not eliminate the buffering of the temperature profile. This result should be expected since the hydrogen reactions only destroy ozone, whereas the production of ozone by reaction 5 is temperature dependent no matter what destruction processes are dominant. Equations (55) and (56) indicate that the ozone density and, thus, the temperature profile above 45 km are dependent on the rate used for reaction 5. The temperature profiles in figure 6, where three different values are used for the rate of reaction 5, show this dependence. Thus the mixing ratio of OH is proportional to the square root of the water vapor mixing ratio. From eq (49), it is apparent that the importance of the hydrogen reactions to the ozone mixing ratio is directly proportional to $B\phi\psi$. Thus increasing the water

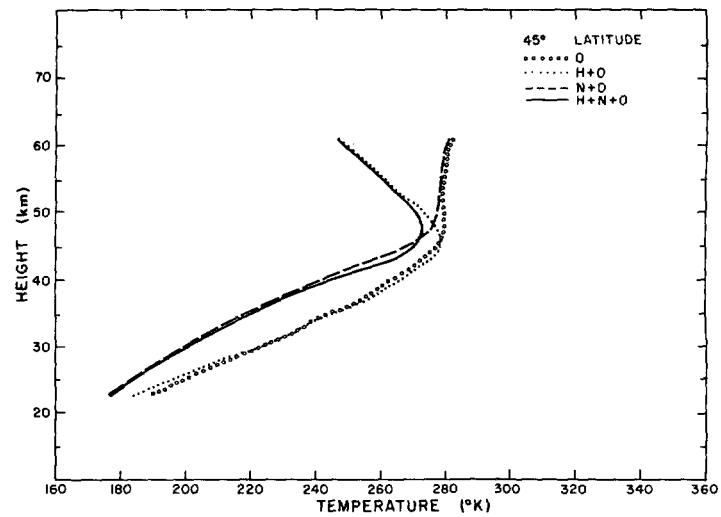

FIGURE 4.—Same as figure 2 except this is for 45° latitude at the equinox.

vapor mixing ratio both increases the importance of the hydrogen reactions at a given height and decreases the height at which the hydrogen reactions become dominant in determining the ozone mixing ratio.

The mixing ratio of OH may be estimated from eq (50) as

$$\psi=\left(\frac{D\phi+G}{E}\right)^{1/2}. \tag{57}$$

The use of eq (30), (31), and (32) in eq (57) gives

$$\psi=\left[\frac{\frac{k_8q_{3b}\phi}{k_7}+q_{H_2O}}{(k_{13}+R_2k_{14})n_m}\right]^{1/2}\left(\frac{n_{H_2O}}{n_m}\right)^{1/2}. \tag{58}$$

Above 45 km, eq (13) may be used for R_2. That is,

$$R_2\approx\frac{k_9}{k_{11}}\left(1+\frac{n_{O_3}k_{27}}{n_{O_2}n_mk_{10}}\right)^{-1}, \tag{59}$$

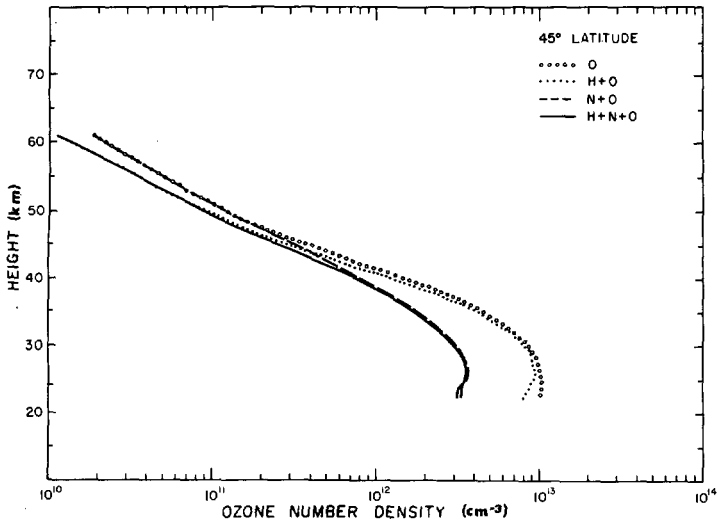

FIGURE 5.—Same as figure 3 except this is for 45° latitude at the equinox.

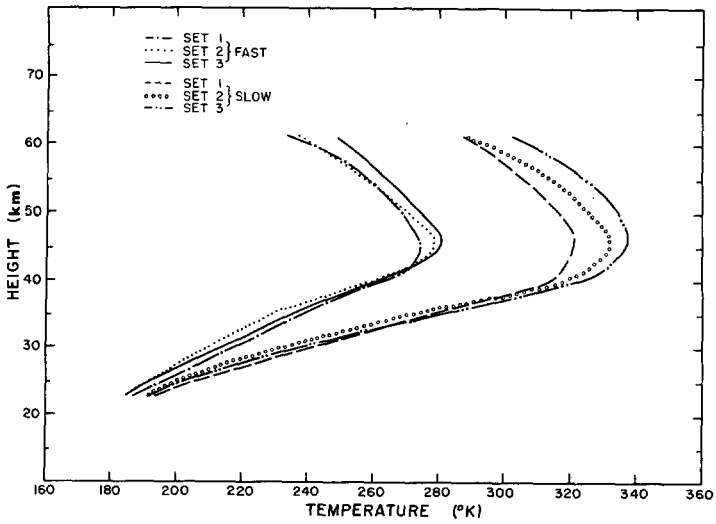

FIGURE 6.—Radiative-photochemical equilibrium temperature as a function of height for 0° latitude for an N + H + O atmosphere. The three sets of reaction rates are in table 2.

and eq (58) becomes

$$\psi \approx \left[\frac{\left(\frac{k_8 q_{3b} \phi}{k_7} + q_{H_2O} \right) k_{11}}{k_9 k_{14} n_m \left(1 + \frac{n_{O_3} k_{27}}{n_{O_2} n_m k_{10}} \right)^{-1}} \right]^{1/2} \left(\frac{n_{H_2O}}{n_m} \right)^{1/2}. \quad (60)$$

Also, above 45 km, we may use an approximate form of eq (33); that is,

$$B \approx 2 R_1 k_9 n_m. \quad (61)$$

Equations (59), (60), and (61) are not used in our radiative photochemical equilibrium calculations; but they are useful in estimating the effect of varying the rates for the hydrogen reactions.

From eq (60), it is apparent that changes in k_8, k_{11}, k_{14}, k_{27}, and k_{10} will be indistinguishable in their effects from changes in the assumed water vapor mixing ratio. The effect of varying the water vapor mixing ratio has been discussed previously. We shall return to this matter later in evaluating our quantitative results.

The effect of the nitrogen reactions on the ozone mixing ratio is indicated in eq (49) by $-F\phi X$. Use of eq (28), (14), and (21) plus the fact that $R_1 k_{16} > k_{18}$ at all heights yields

$$F\phi X \approx \frac{2 R_1 k_{16} n_m K \phi}{1 + R_3}. \quad (62)$$

Using eq (14), we estimate that $R_3 < 1$ below 35 km and $R_3 \approx R_1 k_{16}/k_{17}$ above 35 km. Therefore, below 35 km,

$$F\phi X \approx 2 R_1 k_{16} n_m K \phi; \quad (63)$$

and above 35 km,

$$F\phi X \approx \frac{2 R_1 k_{16} n_m K \phi}{1 + \frac{R_1 k_{16}}{k_{17}}}. \quad (64)$$

From eq (63) and (64), it is apparent that variations in k_{16} or k_{17} may be equivalently expressed as changes in K, the mixing ratio of nitrogen oxides. The effect on the ozone mixing ratio due to varying the nitrogen oxides mixing ratio has already been indicated.

Finally, note that, below 30 km, the photochemical time scale for ozone is so long (several weeks to years) that dynamical effects can be significant. It follows that joint radiative-photochemical equilibrium calculations should not be expected to give results in agreement with observed temperature and ozone density distributions. Above 35 km, both the photochemical time scale (<1 day) and the radiative-photochemical cooling time scale (about a few days) are short enough that dynamical effects are unimportant. Therefore, equilibrium calculations should give appropriate values of ozone density and temperature.

Figures 2–6 clearly show that distributions of temperature and ozone density depend on values used for parameters such as reaction rate coefficients, cooling time scale, and mixing ratios of water vapor and nitrogen oxides. These parameters can be adjusted to yield distributions that best match the observed distributions of ozone density and temperature. Comparison of ozone measurements made by several investigators (Van Allen and Hopfield 1952, Johnson et al. 1954, Rawcliffe et al. 1963, Miller and Stewart 1965, Weeks and Smith 1968, Hilsenrath et al. 1969) shows a range in number density as large as an order of magnitude at some heights in the 35–61 km region. Since the temperature in this region is much better determined as in COESA (1962) or Valley (1965), temperature rather than ozone density is used to determine the match of the equilibrium calculations to observations.

The supplemental atmosphere (tropical) in Valley (1965) has a stratopause temperature of 270°K with 243°K at 35 km and 250°K at 61 km. In fitting the equilibrium

temperature profile to the supplemental atmosphere, we wish to match the stratopause temperature and the slope of the temperature profile above and below the stratopause. In figures 2, 4, and 6, the stratopause temperatures are 270°–285°K for all cases with the fast cooling rate coefficient and 315°–335°K for all cases with the slow cooling rate coefficient [$a=(17\text{ days})^{-1}$]. As previous discussion indicates, the equilibrium temperature at 50 km can be lowered by increasing the water vapor mixing ratio. However, increasing the water vapor mixing ratio also increases the magnitude of the slope of the temperature profile between 50 and 61 km. As figure 6 shows, there is approximately a 30°K decrease in the equilibrium temperature between 50 and 61 km for a water vapor mixing ratio of 1.5×10^{-6} and the slow cooling rate coefficient. Thus increasing the water vapor mixing ratio to lower the 315°–335°K temperature at 50 km will lower the equilibrium temperature far too much at 61 km. Therefore, the fast cooling rate coefficient is used to model the equilibrium temperature. Also, set 3 for the pure oxygen reaction rates is used since this set is most recent.

Temperature profiles in figures 2 and 4 indicate that cases with water vapor absent have a nearly constant temperature above 50 km while cases with a water vapor mixing ratio of 1.5×10^{-6} show a decrease of about 25°K between 52 and 61 km. Larger values for the water vapor mixing ratio exhibit an even larger decrease in equilibrium temperature above 50 km; this larger decrease is unacceptable since the supplemental atmosphere (Valley 1965) has only a 20°K decrease from 50 to 61 km. As eq (60) and (61) indicate, a decrease in the dissociation rates of water vapor, a decrease in k_{11} or k_9, or an increase in k_{14} would mean the water vapor mixing ratio must be increased to maintain the same calculated equilibrium temperature. Thus the water vapor mixing ratio that gives the best fit to the supplementary atmosphere is 1.5×10^{-6} only for those hydrogen reaction rates found in table 1. However, it is necessary to include the water vapor reactions to produce the decline in temperature above 50 km.

Temperature profiles in figures 2 and 4 show that inclusion of the nitrogen reactions reduces the equilibrium temperature below 45 km and has only small effects above 45 km. At 0° latitude, for the nitrogen oxides mixing ratio used (3×10^{-8}), the equilibrium temperature at 35 km is about 238°K as opposed to 265°K when the nitrogen reactions are neglected. The inclusion of the nitrogen reactions is necessary to lower the equilibrium temperature to that of the supplementary atmosphere at 35 km. However, it should be noted in figure 2 that the equilibrium temperature at 46 km is 281°K, which is 14°K higher than the 267°K at the same height in the supplementary atmosphere (tropical). The equilibrium temperature at 46 km can be reduced to 267°K by raising the nitrogen oxides mixing ratio to 10^{-7}. Changing the water vapor mixing ratio does not work since the match at 50 and 61 km would then be removed. A nitrogen oxides mixing ratio of 10^{-7} yields an equilibrium temperature of 224°K at 35 km, which is 20°K lower than the supplementary atmosphere (tropical) has at 35 km. Thus to model the temperature between 35 and 46 km, one must increase the nitrogen oxides mixing ratio from 3×10^{-8} at 35 km to 10^{-7} at 46 km. Above 46 km, the nitrogen reactions have less effect; and very large changes in the nitrogen oxides mixing ratio would yield only small changes in the equilibrium temperature. Below 35 km, we do not expect to model the temperature correctly without including dynamical effects; therefore, no particular value for the nitrogen oxides mixing ratio can be spceified. Finally, from eq (64), it is apparent that the mixing ratio of nitrogen oxides needed to give a particular temperature distribution is altered when the reaction rates k_{16} and k_{17} are altered.

The preceding results, while interesting, are not as important as the fact that the system we have developed is simple enough to permit the immediate evaluation of the effects of various changes and the identification of questionable rate coefficients. We shall now use this simplicity to assess and extend these results.

In the preceding scheme, we have essentially asked what amount of ozone is necessary to produce the observed mean temperature between 35 and 60 km. The amount is less than what one would obtain from simple oxygen chemistry. So we further inquired how much H_2O and NO_x would be needed for the various catalytic destructions of ozone to that needed. We obtained answers to these questions for the reaction rates and cooling rate coefficients used. The density of ozone calculated is within the range of the few existing observations. Near the upper limit, however, the results are questionable on at least two counts:

1. The suggested mixing ratio for NO_x at 50 km (1×10^{-7}) is higher than has hitherto been suggested.
2. The mixing ratio for H_2O suggested (1.5×10^{-6}) is less than currently believed.

As noted previously, the mixing ratios needed to produce given temperature and ozone distributions may be changed when reaction rates are changed. However, for the sake of illustration, let us consider a change in another parameter, the cooling rate coefficient, a. The value of a at 50 km for the fast profile is $a=(4.63\text{ days})^{-1}$, which is larger than most previously used values. Suppose a is reduced to $a=(5.79\text{ days})^{-1}$. From eq (51), it is obvious that the amount of ozone must be reduced by 20 percent to maintain the same temperature. This reduction still leaves the ozone number density within the range of the observations.

With 20 percent less ozone at 50 km, the loss terms due to hydrogen and nitrogen reactions must be increased in eq (49). For this example, the reaction rates are assumed correct; therefore, this can be achieved by increasing the mixing ratios for NO_x and H_2O. Since our value for the mixing ratio of nitrogen oxides is already large, only the latter possibility is considered. To allow for 20 percent less ozone, we must increase the mixing ratio for water vapor from 1.5×10^{-6} to 5.4×10^{-6}. This larger value is within the range of observations (Mastenbrook 1968, Schölz 1970).

TABLE 3.—*Values for the variables used in eq (49) and (51) for the N+H+O case shown in figures 2 and 3 (case I) and for the case with the reduced cooling rate coefficient (case II).*

	Case I	Case II
B	2.86×10^{5} s^{-1}	2.86×10^{5} s^{-1}
F	5.20×10^{4} s^{-1}	5.20×10^{4} s^{-1}
ϕ	4.12×10^{-6}	3.30×10^{-6}
a	2.5×10^{-6} s^{-1}	2.0×10^{-6} s^{-1}
η_{H_2O}/n_m	1.5×10^{-6}	5.4×10^{-6}
K	3.00×10^{-8}	3.00×10^{-8}
C	5.61×10^{-10} s^{-1}	5.61×10^{-10} s^{-1}
X	2.38×10^{-10}	2.38×10^{-10}
ψ	2.28×10^{-10}	3.88×10^{-10}
R_1	0.140	0.140
R_2	1.00	1.00
R_3	125	125
A	14.2 s^{-1}	14.2 s^{-1}
T	270°K	270°K
η	114.2 °K/s	114.2°K/s

The reader may verify the results described in the preceding two paragraphs or determine the effect of changing other parameters by using table 3. In this table, the values at 50 km are given for the quantities found in eq (49) and (51). Case I is the N+H+O case shown in figures 2 and 3, and case II is that just discussed with the cooling rate coefficient, a, reduced to $(5.79\ \text{days})^{-1}$.

It appears that a plausible choice for the NO_x mixing ratio between 35 and 50 km is $3\text{–}10\times10^{-8}$. This is considerably more than what is expected will be produced by full scale supersonic transport (SST) operations (Johnston 1972). The SST fleets will be operating at 20 km, whereas the mixing ratios have been found for the region where photochemical equilibrium obtains (above 35 km). Indeed, it is the region above about 30 km that is the primary photochemical source and sink region for lower levels, which are coupled to the higher levels through hydrodynamic transport. NO_x deposited at SST levels will probably be converted to HNO_3 and HNO_2; however, the HNO_3 and HNO_2 may then be transported upward to levels where they will be photodissociated yielding NO_x again. The change in NO_x at heights of rapid chemistry due to SST's may be on the order of 5 percent of our estimated ambient NO_x. At these heights, a change of 5 percent in NO_x should not produce a similar change in ϕ since nitrogen reactions are not the only loss processes for ozone and also because of the thermal buffering, which we have previously discussed.

5. RELAXATION TIME SCALES

Suppose we consider small perturbations from the radiative-photochemical equilibrium state calculated in section 4. Only local perturbations are considered. That is, we are asking how the system behaves if it is perturbed from equilibrium at one height while equilibrium conditions exist at other heights. Then linearization of eq (22) and (23) yields equations that can be solved for the time scales for return to radiative-photochemical equilibrium. With winds neglected, the equations are

$$\frac{\partial\phi'}{\partial t}=-\mathcal{B}\phi'-\mathcal{C}\psi'-\mathcal{G}T', \tag{65}$$

$$\frac{\partial\psi'}{\partial t}=\mathcal{D}\phi'-\mathcal{E}\psi'-\mathcal{F}T', \tag{66}$$

and

$$\frac{\partial T'}{\partial t}=\eta\phi'-aT' \tag{67}$$

where (using primes for perturbation quantities and overbars for equilibrium value)

$$\phi=\bar{\phi}+\phi',$$

$$\psi=\bar{\psi}+\psi',$$

$$T=\bar{T}+T',$$

$\frac{n_m'}{\bar{n}_m}\approx\frac{T'}{\bar{T}}$ (valid for small pressure perturbations),

$$\mathcal{B}=\frac{2\overline{A\phi}+\overline{B\psi}(1+\delta_1)+\overline{FX}(1+\epsilon_1)}{1+R_1}, \tag{68}$$

$$\mathcal{C}=\frac{\overline{B\phi}}{1+R_1}, \tag{69}$$

$$\mathcal{G}=\frac{\frac{\bar{\phi}}{\bar{T}}[\alpha\overline{A\phi}+(\beta-\delta_2\epsilon_2)\overline{B\psi}+(f+\epsilon_2)\overline{FX}]}{1+R_1}, \tag{70}$$

$$\mathcal{D}=\frac{\overline{D}-\frac{g\overline{E\psi}^2}{\bar{\phi}}}{1+R_2}, \tag{71}$$

$$\mathcal{E}=\frac{2\overline{E\psi}}{1+R_2}, \tag{72}$$

and

$$\mathcal{F}=\frac{\frac{r\overline{E\psi}^2}{\bar{T}}}{1+R_2}. \tag{73}$$

Further definitions are

$$\alpha=1+e_6-e_5,$$

$$\gamma_4=\gamma_1+\gamma_2,$$

$$\gamma_1=\frac{\frac{k_{16}k_{15}}{k_{17}\bar{\phi}}\bar{X}}{k_{11}+\frac{R_3\bar{X}k_{15}}{R_1\bar{\phi}}},$$

$$\gamma_2=\frac{\frac{k_{15}\bar{X}q_{NO_2}}{R_1\bar{\phi}^2\bar{n}_mk_{17}}}{k_{11}+\frac{R_3\bar{X}k_{15}}{R_1\bar{\phi}}},$$

$$\omega=\frac{k_{12}}{k_{12}+R_1k_9}[e_{12}-(2-e_5)]-\gamma_1(e_{15}+e_{16}-e_{17})$$
$$-\gamma_2[e_{15}+1-e_{17}-(2-e_5)],$$

$$\epsilon_1=\frac{q_{NO_2}}{(1+R_3)(\bar{\phi}\bar{n}_mk_{17})},$$

$$\epsilon_2=-\frac{R_1k_{16}}{(1+R_3)k_{17}}[e_{16}+(2-e_5)-e_{17}]-\epsilon_1(1-e_{17}),$$

$$g=\gamma_3 \qquad z\leq 40 \text{ km},$$

$$g=-\frac{\Delta}{(1+\Delta)^2}\frac{k_9}{k_{11}}\frac{1}{R_2} \qquad z\geq 40 \text{ km},$$

$$\Delta=\bar{\phi}\frac{k_{27}}{n_{O_2}k_{10}},$$

$$\gamma_3=\gamma_4\left(1+\frac{\epsilon_1}{R_3}\right),$$

$$r=\omega-\epsilon_2\gamma_4-1 \qquad z\leq 40 \text{ km},$$

$$r=-\frac{\Delta}{(1+\Delta)^2}\frac{k_9}{k_{11}R_2}(e_{27}+1)+\frac{k_{12}}{R_1k_{11}R_2}(e_{12}-2+e_5)-1 \qquad z\geq 40 \text{ km},$$

$$f=-1+\frac{2R_1k_{16}(e_{16}+2-e_5)+k_{18}e_{18}}{2R_1k_{16}+k_{18}},$$

$$\beta=-1+\frac{[(k_9+R_2k_{11})(2-e_5)R_1+R_1R_2k_{11}\omega+k_{12}e_{12}]n_m}{\overline{B}},$$

$$\delta_1=\frac{\gamma_3R_1R_2k_{11}n_m}{\overline{B}},$$

$$\delta_2=\frac{\delta_1\gamma_4}{\gamma_3},$$

$$e_i=\frac{\overline{T}}{k_i}\left(\frac{dk_i}{d\overline{T}}\right)_{\overline{T}} \qquad (i=5,\ 18),$$

and [from the linearization of eq (24)]

$$\frac{X'}{\overline{X}}=\epsilon_1\frac{\phi'}{\bar{\phi}}+\epsilon_2\frac{T'}{\overline{T}}.$$

The complexity of our coefficients in eq (65) and (66) arises because some of the reaction rate coefficients, k_i, and the ratios R_1, R_2, and R_3 are temperature dependent and the ratios R_2 and R_3 are also dependent on the ozone mixing ratio. There are additional terms in eq (65) and (66) that have been neglected since they are much smaller than those retained. If there is no coupling, then the time scale for return to equilibrium is $\mathcal{B}^{-1}$ for the ozone mixing ratio, $\mathcal{E}^{-1}$ for the hydroxyl mixing ratio, and a^{-1} for the temperature. The terms $\mathcal{C}\varphi'$, $\mathcal{G}T'$, $\mathcal{D}\phi'$, $\mathcal{F}T'$, and $\eta\phi'$ represent the coupling between the photochemical and radiative processes.

Equations (65), (66), and (67) may be combined to form

$$\left[\frac{\partial^3}{\partial t^3}+M\frac{\partial^2}{\partial t^2}+N\frac{\partial}{\partial t}+S\right]\begin{pmatrix}\phi'\\ \psi'\\ T'\end{pmatrix}=0 \qquad (74)$$

where

$$M=a+\mathcal{B}+\mathcal{E},$$

$$N=\mathcal{B}\mathcal{E}+a\mathcal{B}+\mathcal{E}a+\mathcal{G}\eta+\mathcal{C}\mathcal{D},$$

and

$$S=\mathcal{E}a\mathcal{B}+\eta\mathcal{G}\mathcal{E}+\mathcal{C}a\mathcal{D}-\mathcal{F}\mathcal{C}\eta.$$

Initial conditions are needed to solve eq (74). We consider three cases:

1. $\phi'(t=0)=\phi(0)$,
   $\psi'(t=0)=0$,
   $T'(t=0)=0$,
2. $\phi'(t=0)=0$,
   $\psi'(t=0)=\psi(0)$,
   $T'(t=0)=0$,

and

3. $\phi'(t=0)=0$,
   $\psi'(t=0)=0$,
   $T'(t=0)=T(0)$.

The solution for ϕ' for case 1 is

$$\phi'=\phi(0)K_{11}e^{\sigma_1t}+K_{21}e^{\sigma_2t}+K_{31}e^{\sigma_3t};$$

the solution for ψ' for case 2 is

$$\psi'=\psi(0)K_{12}e^{\sigma_1t}+K_{22}e^{\sigma_2t}+K_{32}e^{\sigma_3t};$$

and the solution for T' for case 3 is

$$T'=T(0)K_{13}e^{\sigma_1t}+K_{23}e^{\sigma_2t}+K_{33}e^{\sigma_3t}.$$

The coefficients are defined as

$$K_{1j}=\frac{\theta_j+V_j(\sigma_2+\sigma_3)+\sigma_2\sigma_3}{(\sigma_1-\sigma_3)(\sigma_1-\sigma_2)},$$

$$K_{2j}=\frac{\theta_j+V_j(\sigma_3+\sigma_1)+\sigma_1\sigma_3}{(\sigma_2-\sigma_3)(\sigma_2-\sigma_1)},$$

and

$$K_{3j}=\frac{\theta_j+V_j(\sigma_1+\sigma_2)+\sigma_1\sigma_2}{(\sigma_3-\sigma_1)(\sigma_3-\sigma_2)}$$

where $j=1,\ 2,\ 3$ and

$$V_1=\mathcal{B},$$
$$V_2=\mathcal{E},$$
$$V_3=a,$$
$$\theta_1=\mathcal{B}^2-\eta\mathcal{G}-\mathcal{C}\mathcal{D},$$
$$\theta_2=\mathcal{E}^2-\mathcal{C}\mathcal{D},$$
$$\theta_3=a^2-\eta\mathcal{G}.$$

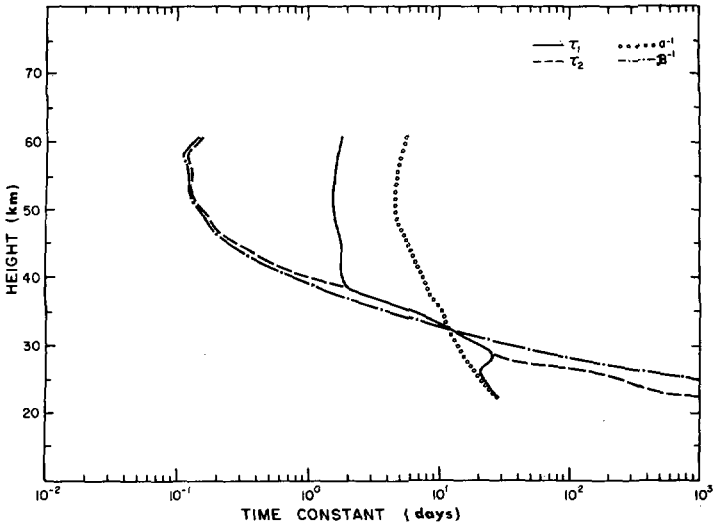

FIGURE 7.—Relaxation time scales in a pure O atmosphere. $\mathcal{B}^{-1}$ and a^{-1} are the relaxation time scales for O_3 and temperature, respectively, when the coupling between the photochemistry and temperature is neglected; τ_2 and τ_1 are the relaxation time-scales for the O_3 and temperature, respectively, when the coupling is considered.

The values σ_1, σ_2, and σ_3 are roots of the cubic equation

$$\sigma^3+M\sigma^2+N\sigma+S=0, \tag{75}$$

which follows from eq (74).

For cases where the hydrogen reactions are neglected, eq (74) reduces to

$$\left[\frac{\partial^2}{\partial t^2}+(a+\mathcal{B})\frac{\partial}{\partial t}+(a\mathcal{B}+\mathcal{G}\eta)\right]\begin{pmatrix}\phi'\\T'\end{pmatrix}=0 \tag{76}$$

with the solution for ϕ' (case 1) as

$$\phi'=\phi(0)\frac{\sigma_2+\mathcal{B}}{\sigma_2-\sigma_1}e^{\sigma_1 t}-\frac{\sigma_1+\mathcal{B}}{\sigma_2-\sigma_1}e^{\sigma_2 t} \tag{77}$$

and the solution for T' (case 3) as

$$T'=T(0)\frac{\sigma_2+a}{\sigma_2-\sigma_1}e^{\sigma_1 t}-\frac{\sigma_1+a}{\sigma_2-\sigma_1}e^{\sigma_2 t} \tag{78}$$

where

$$\sigma_1=\tfrac{1}{2}\{-(a+\mathcal{B})-[(a-\mathcal{B})^2-4\eta\mathcal{G}]^{1/2}\} \tag{79}$$

and

$$\sigma_2=\tfrac{1}{2}\{-(a+\mathcal{B})+[(a-\mathcal{B})^2-4\eta\mathcal{G}]^{1/2}\}. \tag{80}$$

In figure 7, time scales a^{-1}, $\mathcal{B}^{-1}$, $\tau_1[=-(\mathrm{Re}\sigma_1)^{-1}]$, and $\tau_2[=-(\mathrm{Re}\sigma_2)^{-1}]$ are plotted for the pure O case with set 3 for rates of reactions 5 and 6 and the fast profile of a. (Here, Re signifies the real part.) The possibility of complex σ_1 and σ_2 merely means that the coupling results in an oscillating decay of the perturbations. The time scale $\mathcal{B}^{-1}$ is several years at 22 km, decreases to about 90 min at 50 km, and then increases above 50 km to about 1/10 day at 61 km. When coupling is included, the actual time scale for thermal relaxation is τ_1; and that for ozone relaxation is τ_2. As shown in figure 7, coupling results in a slightly more rapid ozone relaxation below 30 km and a slightly slower ozone relaxation above 30 km.

Below 30 km, coupling appears to cause a slower thermal relaxation; however, as shown below, this is not the case if we are considering short period waves ($\tau<a^{-1}$). If we write eq (79) and (80) as

$$\sigma_1=-\frac{(a+\mathcal{B})}{2}-\frac{\delta}{2} \tag{81}$$

and

$$\sigma_2=-\frac{(a+\mathcal{B})}{2}+\frac{\delta}{2} \tag{82}$$

where

$$\delta\equiv[(a-\mathcal{B})^2-4\mathcal{G}\eta]^{1/2}$$

and then substitute eq (81) and (82) into eq (78), the result is

$$T'=\frac{T(0)}{2\delta}e^{-\frac{(a+B)t}{2}}[(\mathcal{B}-a)(e^{(\delta/2)t}-e^{-(\delta/2)t})+\delta(e^{(\delta/2)t}+e^{-(\delta/2)t})]. \tag{83}$$

Now, $\delta/2<(a+\mathcal{B})/2$; and if we consider an expansion of $e^{\pm(\delta/2)t}$ for time less than $(\delta/2)^{-1}$, we then may write eq (83) as

$$T'\approx T(0)e^{-\frac{(a+B)}{2}t}\left[1-\frac{(a-\mathcal{B})}{2}t\right] \tag{84}$$

or

$$T'\approx T(0)e^{-at}. \tag{85}$$

Thus if we are considering a wave with period $\tau<a^{-1}$, then the actual time scale for thermal relaxation is not τ_1 but a^{-1} below 30 km where eq (84) and (85) are good approximations to eq (83).

Above 30 km, $\mathcal{B}^{-1}$ is much less than a^{-1}; and coupling between the photochemical and radiative processes results in more rapid thermal relaxation as shown in figure 7. Lindzen and Goody (1965) also found that thermal relaxation was more rapid above 30 km, though they used a different set of rate coefficients for reactions 5 and 6.

Above 40 km,

$$4(\mathcal{G}\eta+a\mathcal{B})\ll(a+\mathcal{B})^2,$$

and

$$\mathcal{B}^{-1}\ll a^{-1};$$

therefore, eq (81) can be approximated by

$$\sigma_1\approx-\frac{\mathcal{G}\eta}{\mathcal{B}}. \tag{86}$$

For the pure O case, eq (68) and (70) reduce to

$$\mathcal{B}=2A\bar{\phi} \tag{87}$$

and

$$\mathcal{G}=\alpha\bar{A}\bar{\phi}\frac{\bar{\phi}}{\bar{T}}. \tag{88}$$

Use of eq (87) and (88) in eq (86) yields

$$\sigma_1\approx-\frac{\alpha A\eta\bar{\phi}}{2A\bar{\phi}}\frac{\bar{\phi}}{\bar{T}}=-\frac{\alpha\eta\bar{\phi}}{2\bar{T}}. \tag{89}$$

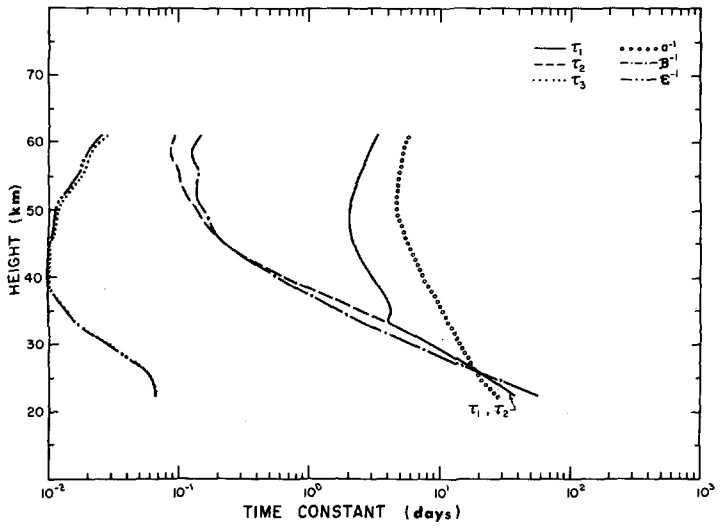

FIGURE 8.—Relaxation time scales in an N + H + O atmosphere. $\mathcal{B}^{-1}$, $\mathcal{E}^{-1}$, and a^{-1} are the relaxation time scales for O_3, OH, and temperature, respectively, when the coupling between the photochemistry and temperature is neglected. The variables τ_2, τ_3, and τ_1 are the relaxation time scales for O_3, OH, and temperature, respectively, when the coupling is included.

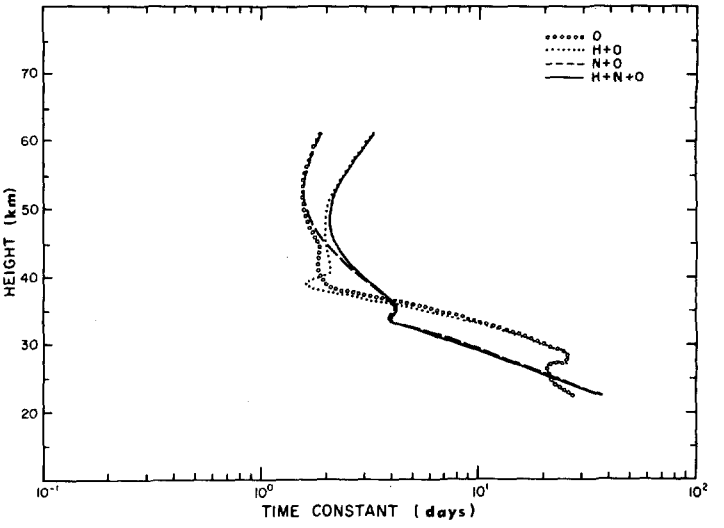

FIGURE 9.—Thermal relaxation time scale, τ_1, as a function of height for the cases considered in figures 2 and 3.

Substitution of eq (51) into eq (89) gives

$$\sigma_1 \approx -\frac{\alpha a}{2}\left(1-\frac{\bar{b}}{\bar{a}\bar{T}}\right). \tag{90}$$

From figures 2 and 4, we see that the equilibrium temperature for the pure O case is nearly constant above 40 km; therefore [from eq (90)], σ_1 is nearly constant above 40 km as shown in figure 7.

The N+H+O case requires the solution of eq (75). Figure 8 shows the values a^{-1}, $\mathcal{B}^{-1}$, and $\mathcal{E}^{-1}$ as well as τ_1, τ_2, and τ_3 [$=-(\mathrm{Re}\sigma_3)^{-1}$] where τ_3 is the hydroxyl relaxation time scale when coupling is included. Set 3 is used for rate coefficients for reactions 5 and 6, and the fast profile is used for a. The water vapor mixing ratio is 1.5×10^{-6}, and the mixing ratio for the nitrogen oxides is 3×10^{-8}. In figure 8 we see that, below 40 km, $\tau_3 \approx \mathcal{E}^{-1}$ and τ_1 and τ_2 are approximately the same as for the pure O case. This result is reasonable since we previously found that inclusion of the hydrogen reactions has little effect on the equilibrium distribution of temperature and ozone density below 40 km. The only effect of the nitrogen reactions is to shorten $\mathcal{B}^{-1}$ at the lowest altitudes.

Above 40 km, the hydrogen reactions become increasingly important as $\mathcal{E}^{-1}$ increases while $\mathcal{B}^{-1}$ decreases. The time scale for relaxation of a perturbation in the ozone density or hydroxyl density is modified since there is strong coupling between the ozone and hydrogen photochemistry. The photochemical acceleration of the thermal relaxation is modified but not eliminated. Above 40 km, eq (86) is applicable; and

$$\sigma_1 \approx -\frac{\mathcal{G}\eta}{\mathcal{B}}. \tag{91}$$

For the N + H + O case above 45 km, eq (68) and (70) reduce to

$$\mathcal{B} \approx B\bar{\psi} \tag{92}$$

and

$$\mathcal{G} \approx \beta B\bar{\psi}\frac{\bar{\phi}}{\bar{T}}. \tag{93}$$

Thus substitution of eq (92), (93), and (51) into eq (91) yields

$$\sigma_1 \approx -\beta\eta\frac{\bar{\phi}}{\bar{T}} = -\beta a\left(1-\frac{\bar{b}}{\bar{a}\bar{T}}\right). \tag{94}$$

As pointed out in section 4, the pure oxygen reactions still make a sizable contribution to the destruction of ozone up to 52 km. However, eq (92) and (93) are used to illustrate explicitly what effect the hydrogen chemistry has on the resulting time scales. A comparison of eq (90) and eq (94) shows that the expressions for σ_1 for the pure oxygen reactions and for the hydrogen reactions differ by $\alpha/2$ in the first and β in the second. The quantities $\alpha/2$ and β merely express the temperature dependence of ozone destruction due to pure oxygen reactions and to hydrogen reactions, respectively. At 50 km, for example, $\alpha/2 \approx 6$ while $\beta \approx 3$. Thus the hydrogen reactions do have a smaller temperature dependence, but this dependence is not negligible above approximately 45 km where the hydrogen reactions are important to the ozone destruction. The fact that hydrogen reactions have a smaller temperature dependence than the pure oxygen reactions is clearly illustrated in figure 9 where the time scales for thermal relaxation, τ_1, are longer above 45 km for cases with the hydrogen reactions included. However, the cases with hydrogen reactions included still have $\tau_1 < a^{-1}$, which shows that the temperature dependence of these reactions is sufficient for photochemical acceleration of the thermal relaxation to occur. Finally, the equilibrium temperature for the N + H + O case in figure 2 decreases nearly linearly with height above 50 km while a also decreases.

From eq (94), it is apparent that both of these decreases cause τ_1 to increase above 50 km as shown in figure 8.

Figure 9 shows τ_1 for four cases (O, H+O, N+O, and H+N+O). It is apparent that inclusion of the nitrogen reactions causes a decrease in τ_1 between 36 and 25 km and an increase in τ_1 below 25 km and between 36 and 44 km. The last result can be explained most readily by referring to the equilibrium eq (49), (50), and (51). The effect of nitrogen reactions on ozone density is contained in the term $-F\phi X$; and above 35 km, this term can be written [by application of eq (29), (14), and (9)] as

$$FX\phi \approx 2k_{17}K\phi n_m. \tag{95}$$

The effect of the pure oxygen reactions on ozone density is contained in the term $-A\phi^2$; and from eq (26) and (9), we have

$$A\phi^2 = \frac{2(q_{3a}+q_{3b})}{n_{O_2}} \frac{k_6}{k_5} \phi^2. \tag{96}$$

Comparing eq (95) and (96), we see that temperature dependence of ozone density due to nitrogen reactions is by k_{17} and the temperature dependence of ozone density due to the oxygen reactions is by $(k_6/k_5)^{1/2}$. The temperature dependence of k_{17} is much less than that of $(k_6/k_5)^{1/2}$. Thus the temperature dependence of $F\phi X$ is less than that of $A\phi^2$. Between 36 and 45 km, the nitrogen reactions as well as the pure oxygen reactions are important in determing the ozone density. Since the temperature dependence of $F\phi X$ is less than that of $A\phi^2$, it follows that including the nitrogen reaction increases τ_1 from the value found when only the pure oxygen reactions are included. (The hydrogen reactions are unimportant below 45 km for the mixing ratio used.)

Between 25 and 36 km for all cases plotted in figure 9, the time scale for cooling by the 15-μm band of CO_2, a^{-1}, and the photochemical relaxation time scale for ozone (neglecting coupling), $\mathcal{B}^{-1}$, are comparable in size. Therefore, $a-\mathcal{B}$ is small; and [referring to eq (79) and (80)] $(a-\mathcal{B})^2 < 4\eta\mathcal{G}$. Since $\tau_1 = \mathrm{Re}-(\sigma_1)^{-1}$,

$$\tau_1 \approx \frac{2}{a+\mathcal{B}}$$

in this height range. The fast value for a is used for all cases in figure 9. In this height range, however, cases with nitrogen reactions included have shorter photochemical relaxation time scales, $\mathcal{B}^{-1}$, than cases without the nitrogen reactions included. Thus τ_1 is shorter when the nitrogen reactions are included.

Below 25 km, the photochemical relaxation time scale, $\mathcal{B}^{-1}$, increases for all cases and is longer than the time scale for cooling, a^{-1}. For the cases with nitrogen reactions included, $a-\mathcal{B}$ is still small; and $\tau_1 \approx 2/(a+\mathcal{B})$ as described in the preceding paragraph. Since $\mathcal{B}^{-1} > a^{-1}$,

$$\tau_1 > a^{-1}.$$

However, for cases with nitrogen reactions neglected, $\mathcal{B}^{-1}$ becomes so long that the coupling between photochemistry and temperature is negligible. When coupling is negligible, the thermal relaxation time scale is just the time scale for cooling; or $\tau_1 \approx a^{-1}$. Obviously, below 25 km the inclusion of nitrogen reactions increases the thermal relaxation time scale as compared to values found when no nitrogen reactions are included.

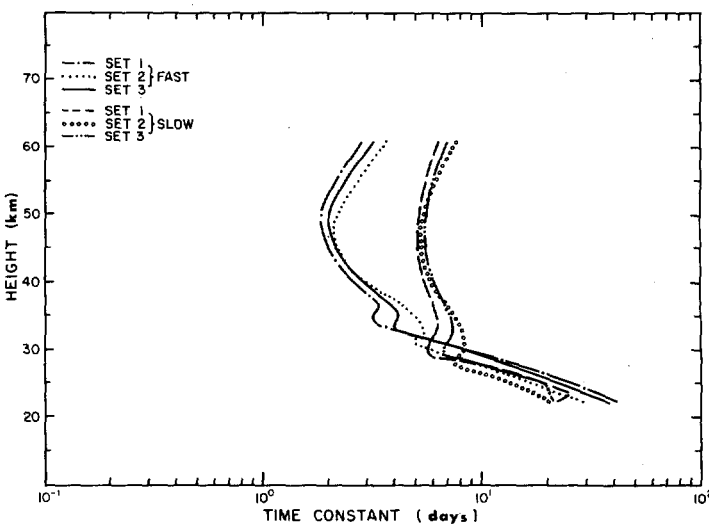

FIGURE 10.—Thermal relaxation time scale, τ_1, as a function of height for the cases considered in figure 6.

Figure 10 shows τ_1 for the N+H+O case when three different sets of rates for reactions 5 and 6 and the two values for a (fast and slow) are used. Above 45 km, eq (90) and (94) both indicate

$$\sigma_1 \approx -\mathcal{K}a\left(1-\frac{\frac{b}{a}}{\overline{T}}\right) \tag{97}$$

where $\mathcal{K}$ is β if the hydrogen reactions dominate and $\mathcal{K}$ is between $\alpha/2$ and β if the pure oxygen reactions are also significant in the ozone destruction in this region. Since the equilibrium temperature varies with different sets of rates for reactions 5 and 6 (fig. 7), so does σ_1.

As discussed in section 4, the effect of varying rates for reactions 7–18 can be shown by varying the water vapor mixing ratio or the mixing ratio of nitrogen oxides. Resulting values of τ_1 are within the range of those shown in figures 9 and 10.

The results show that coupling between radiative and photochemical processes leads to an acceleration of thermal relaxation above 36 km for a wide range of reaction rates and other parameters. The minimum value of τ_1 is between 1.5 and 2 days at 45–50 km for fast a and between 4.5 and 6 days at 34–50 km for slow a. When the hydrogen reactions are neglected, τ_1 is nearly constant above 50 km; when the hydrogen reactions are included with a water vapor mixing ratio of 1.5×10^{-6}, τ_1 increases with height above 50 km from a value of 2 days at 50 km to a value of 3.3 days at 61 km for fast a. Therefore, the Newtonian cooling rate coefficient to be used in the temperature equation for dynamical problems in the stratosphere above 36 km is not a but τ_1^{-1}. Moreover, τ_1^{-1} seems large enough to dissipate internal Rossby waves.

6. CONCLUSIONS

In this paper, we have developed quantitatively justifiable simple models for the radiative heating and the complicated ozone photochemistry of the stratosphere between about 20 and 60 km. These models permit the immediate evaluation of the effects of various chemical and physical quantities on the temperature and ozone distributions in the stratosphere. It should be emphsized that a major difference in our scheme from other simplified schemes is that ours is a *joint radiative-photochemical* model. A purely photochemical model can lead to ozone densities that are in the range of observations but which, if used in the energy equation, lead to temperatures greatly different from those observed. Since the temperature profile at 35–60 km is determined much better than the ozone density distribution, it is obviously preferable to use the equilibrium temperature profile to check the effect of varying mixing ratios and reaction rates. We show that the region 35–60 km should (away from Arctic regions) be in approximately joint radiative-photochemical equilibrium, and we use our simple models to calculate this equilibrium. We show that the interaction of radiation and chemistry significantly buffers the temperature and ozone distributions in the stratosphere so that rather large changes in cooling rates and reaction rates lead to much more modest changes in ozone and temperature. We also show that, given an observed distribution of mean temperature, we can (assuming accurate knowledge of reaction and infrared cooling rate coefficients) determine the amounts of water vapor and nitrogen oxides needed to produce the ozone distribution, which would in turn lead to the observed temperature. This procedure is facilitated by the fact (which we demonstrate) that hydrogen reactions are significant loss processes for ozone above 45 km while nitrogen reactions are important below 50 km. Thus there are regions where nitrogen and hydrogen reactions are individually rather than jointly important. Unfortunately, reaction and cooling rate coefficients are not accurately known. However, our simplified equations can still be used as diagnostic tools. In this manner, we show that an internally consistent description of observed distributions of temperature and ozone in the stratosphere can be obtained with a time scale for infrared cooling varying from 10 days at 35 km to 4.63 days at 50 km, a mixing ratio for nitrogen oxides ($NO+NO_2$) of about $3–10\times10^{-8}$, and a mixing ratio for water of about $1.5–5\times10^{-6}$. The question of normal NO_x mixing ratio has assumed considerable importance recently because it is believed that proposed SST operations may add about 1×10^{-9} to the NO_x mixing ratio. The present calculations suggest that the SST contribution will be only 3–5 percent of the ambient amount; and because of the thermal buffering of the system, the effect of this addition on ozone density should be less than 3–5 percent.

We also used our simple models to calculate the joint radiative-photochemical relaxation of perturbations in temperature, ozone mixing ratio, and hydroxyl mixing ratio away from their equilibrium values. We find that, for all photochemical models considered, the photochemistry greatly accelerates thermal relaxation as calculated simply on the basis of infrared cooling. The time scale for the latter is about 4.63–10 days. The actual time scale for thermal relaxation when photochemistry (which is temperature dependent) is included proves to be only 1.5–2.2 days. These shorter scales imply greatly enchanced damping for hydrodynamic waves in the stratosphere.

ACKNOWLEDGMENTS

The bulk of this work has been supported by Grant GA–25904 of the National Science Foundation and Grant NGR 14–001–193 of the National Aeronautics and Space Administration, both at the University of Chicago. Additional support was received under grant NSF GA 3399OX of the National Science Foundation at Harvard University. Computations were performed at the National Center for Atmospheric Research, which is supported by the National Science Foundation. Useful conversations with S. Wofsy are also gratefully acknowledged.

REFERENCES

Anderson, J. G., and Kaufman, F., "Kinetics of the Reaction $OH(v=0)+O_3\rightarrow HO_2+O_2$," *Chemical Physics Letters*, Vol. 19, Apr. 15, **1973**, pp. 483–487.

Anderson, J. G., Margitan, J. J., and Kaufman, F., "Gas Phase Recombination of OH With NO and NO_2" (submitted to Journal of Chemical Physics, **1973**).

Barth, Charles A., "Nitric Oxide in the Upper Atmosphere," *Annales de Geophysique*, Vol. 22, No. 2, Lille, France, April–June **1966**, pp. 198–207.

Benson, Sidney W., and Axworthy, Arthur E., "Reconsideration of the Rate Constants From the Thermal Decomposition of Ozone," *Journal of Chemical Physics*, Vol. 42, No. 7, Apr. 1, **1965**, pp. 2614–2615.

Berces, T., and Forgeteg, S., "Kinetics of Photolysis of Nitric Acid Vapour, Part 2, Decomposition of Nitric Acid Vapour Photosensitized by Nitrogen Dioxide," *Transactions of the Faraday Society*, Vol. 66, No. 567, Part 3, London, England, Mar. **1970**, pp. 640–647.

Brinkmann, R. T., "Dissociation of Water Vapor and Evolution of Oxygen in the Terrestrial Atmosphere," *Journal of Geophysical Research*, Vol. 74, No. 23, Oct. 20, **1969**, pp. 5355–5368.

Brinkmann, R. T., Green, A. E. S., and Barth, Charles A., "A Digitalized Solar Ultraviolet Spectrum," *Technical Report* No. 32–351, Jet Propulsion Laboratory, California Institute of Technology, Pasadena, Calif., Aug. 15, **1966**, 73 pp.

COESA, U.S. Committee on Extension to the Standard Atmosphere, *U.S. Standard Atmosphere, 1962*, Environmental Science Services Administration (ESSA), National Aeronautics and Space Administration (NASA), and United States Air Force (USAF), Washington, D.C., Dec. **1962**, 278 pp.

Crutzen, Paul J., "Ozone Production Rates in an Oxygen-Hydrogen-Nitrogen Oxide Atmosphere," *Journal of Geophysical Research, Oceans and Atmospheres*, Vol. 76, No. 30, Oct. 20, **1971**, pp. 7311–7327.

Davis, Douglas D., Herron, John T., and Huie, Robert E., "Absolute Rate Constants for the Reaction $O(^3P)+NO_2\rightarrow NO+O_2$ Over the Temperature Range 230°–339°K," *Journal of Chemical Physics*, Vol. 58, No. 2, Jan. 15, **1973**, pp. 530–535.

Dickinson, Robert E., "Vertical Propagation of Planetary Rossby Waves Through an Atmosphere With Newtonian Cooling," *Journal of Geophysical Research*, Vol. 74, No. 4, Feb. 15, **1969**, pp. 929–938.

Dickinson, Rober E., "Method of Parameterization for Infrared Cooling Between the Altitudes of 30 and 70 Kilometers," *Journal of Geophysical Research, Oceans and Atmospheres*, Vol. 78, No. 21, July 20, **1973**, pp. 4451–4457.

Donovan, R. J., and Husain, D., "Recent Advances in the Chemistry of Electronically Excited Atoms," *Chemical Reviews*, Vol. 70, No. 4, Aug. **1970**, pp. 489–516.

Dütsch, H. U., "The Photochemistry of Stratospheric Ozone," *Quarterly Journal of the Royal Meteorological Society*, Vol. 94, No. 402, London, England, Oct. **1968**, pp. 483–497.

Foner, S. N. and Hudson, R. L., "Mass Spectrometry of Inorganic Free Radicals," *Advances in Chemistry*, Series 36, **1962**, pp. 34–49.

Garvin, D., "The Reaction of Oxygen Atoms with Ozone," *Chemical Kinclics Data Survey, N.B.S. Report* 10828, National Bureau of Standards, U.S. Department of Commerce, Gaithersburg, Md., Apr. **1972**, 108 pp.

Greiner, N. R., "Hydroxal Radical Kinetics by Kinetic Spectroscopy, III; Reactions With H_2O_2 in the Range 300°–458°K," *Journal of Physical Chemistry*, Vol. 72, No. 2, Feb. **1968**, pp. 857–859.

Griggs, M., "Absorption Coefficients of Ozone in the Ultraviolet and Visible Regions," *Journal of Chemical Physics*, Vol. 49, No. 2, July 15, **1968**, pp. 857–859.

Hall, T. C., Jr., and Blacet, F. E., "Separation of the Absorption Spectra of NO_2 and N_2O_4 in the Range 2400–5000 Å," *Journal of Chemical Physics*, Vol. 20, No. 11, Nov. **1952**, pp. 1745–1749.

Herron, J. T., and Huie, R. E., "The Reaction Between NO and ^{3}," *Chemical Kinclics Data Survey, N.B.S. Report* 19828, National Bureau of Standards, U.S. Department of Cogmerce, Gaithersburg, Md., Apr. **1972**, 108 pp.

Hilsenrath, Ernest, Seiden, Lester, and Goodman, Philip, "An Ozone Measurement in the Mesosphere and Stratosphere by Means of a Rocket Sonde," *Journal of Geophysical Research, Oceans and Atmospheres*, Vol. 74, No. 28, Dec. 20, **1969**, pp. 6873–6880.

Hinteregger, H. E., "The Extreme Ultraviolet Solar Spectrum and Its Variation During a Solar Cycle," *Annales de Geophysique*, Vol. 26, No. 2, Lille, France, April–June **1970**, pp. 547–554.

Hochanadel, C. J., Ghormley, J. A., and Orgren, P. J., "Absorption Spectrum and Reaction Kinetics of the HO_2 Radical in the Gas Phase," *Journal of Chemical Physics*, Vol. 56, No. 9, May 1, **1972**, pp. 4426–4432.

Holt, R. B., McLane, C. K., and Oldenberg, O., "Ultraviolet Absorption Spectrum of Hydrogen Peroxide," *Journal of Chemical Physics*, Vol. 16, No. 3, Mar. **1948**, pp. 225–229.

Holton, James R., *Introduction to Dynamic Meteorology*, Academic Press, New York, N.Y., **1972**, 319 pp.

Hudson, R. D., Carter, V. L., and Breig, E. J., "Predissociation in the Schumann-Runge Band System of O_2: Laboratory Measurements and Atmospheric Effects," *Journal of Geophysical Research, Space Physics*, Vol. 74, No. 16, Aug. 1, **1969**, pp. 4079–4087.

Huie, Robert E., Herron, John T., and Davis, Douglas D., "Absolute Rate Constants for the Reaction $O+O_2+M \rightarrow O_3+M$ Over the Temperature Range 200°–346°K," *Journal of Physical Chemistry*, Vol. 76, No. 19, **1972**, pp. 2653–2658.

Hunt, B. G., "Photochemistry of Ozone in a Moist Atmosphere,' *Journal of Geophysical Research*, Vol. 71, No. 5, Mar. 1, **1966**, pp. 1385–1398.

Inn, Edward C. Y., and Tanaka, Yoshio, "Absorption Coefficient of Ozone in the Ultraviolet and Visible Regions," *Journal of the Optical Society of America*, Vol. 43, No. 10, Oct. **1953**, pp. 870–873.

Jefferys, Sir Harold, "The Instability of a Compressible Fluid Heated Below," *Proceedings of the Cambridge Philosophical Society*, Vol. 26, Part 2, London, England, Apr. **1930**, pp. 170–172

Johnson, Francis S., Purcell, James D., and Tousey, Richard, "Studies of the Ozone Layer Above New Mexico," *Rocket Exploration of the Upper Atmosphere*, Pergamon Press, London, England, **1954**, pp. 189–199.

Johnston, Harold, "Laboratory Chemical Kinetics as an Atmospheric Science," *Proceedings of the Survey Conference, February* 15–16, 1972, *Climatic Impact Assessment Program, Cambridge, Mass.*, Department of Transportation *Report* DOT-TSC-OST-72-13 Department of Transportation, Washington, D.C., **1972**, pp. 90–114.

Johnston, Harold S., and Yost, Don M., "The Kinetics of the Rapid Gas Reaction Between Ozone and Nitrogen Dioxide," *Journal of Chemical Physics*, Vol. 17, No. 4, Apr. **1949**, pp. 386–392.

Junge, C. E., "Gases," *Air Chemistry and Radioactivity*, Vol. 4, Academic Press, New York, N.Y. **1963**, chapter 1, p. 37.

Kaufman, Frederick, "Neutral Reactions Involving Hydrogen and Other Minor Constituents," *Canadian Journal of Chemistry*, Vol. 47, No. 10, Ottawa, Canada, May 15, **1969**, pp. 1917–1926.

Kondrat'ev, K. Ia., *Radiation in the Atmosphere*, International Geophysics Series, Vol. 12, Academic Press, New York, N.Y., **1969**, 912 pp.

Leovy, Conway B., "Atmospheric Ozone: An Analytic Model for Photochemistry in the Presence of Water Vapor," *Journal of Geophysical Research*, Vol. 74, No. 2, Jan. 15, **1969**, pp. 417–426.

Leovy, Conway B., "Radiative Equilibrium of the Mesosphere," *Journal of The Atmospheric Sciences*, Vol. 21, No. 3, May **1964**a, pp. 238–248.

Leovy, Conway B., "Simple Models of Thermally Driven Mesospheric Circulation," *Journal of the Atmospheric Sciences*, Vol. 21, No. 4, July **1964**b, pp. 327–341.

Lindzen, Richard S. and Blake, Donna, "Internal Gravity Waves in Atmospheres with Realistic Dissipation and Temperature Part II. Thermal Tides Excited Below the Meospause," *Geophysical Fluid Dynamics*, Vol. 2, No. 1, Jan. **1971**, pp. 31–61.

Lindzen, Richard S., and Goody, Richard, "Radiative and Photochemical Processes in Mesospheric Dynamics: Part I, Models for Radiative and Photochemical Processes," *Journal of the Atmospheric Sciences*, Vol. 22, No. 4, July **1965**, pp. 341–348.

Mastenbrook, H. J., "Water Vapor Distribution in the Stratosphere and High Troposphere," *Journal of the Atmospheric Sciences*, Vol. 25, No. 2, Mar. **1968**, pp. 299–311.

McConnell, J. C., and McElroy, M. B., "Odd Nitrogen in the Atmosphere" *Journal of the Atmospheric Sciences*, Vol. 30, No. 8, Nov. **1973**, pp. 1465–1480.

Miller, D. E., and Stewart, K. H., "Observations of Atmospheric Ozone," *Proceedings of the Royal Society of London*, Series A, Vol. 288, No. 1415, England, Nov. 30, **1965**, pp. 540–544.

Morris, E. D., Jr., and Niki, H., "Mass Spectrometric Study of the Reactions of Nitric Acid with O Atoms and H Atoms," *Journal of Physical Chemistry*, Vol. 75, No. 20, **1971**, pp. 3193–3194.

Murcray, David G., Kyle, T. G., Murcray, F. H., and Williams, W. J., "Presence of HNO_3 in the Upper Atmosphere," *Journal of the Optical Society of America*, Vol. 59, No. 9, Sept. **1969**, pp. 1131–1134.

Murgatroyd, R. J., "The Structure and Dynamics of the Stratosphere," *The Global Circulation of the Atmosphere*, G. A. Corby (Editor), Royal Meteorological Society, London, England, **1970**, pp. 159–195.

Murgatroyd, R. J., and Goody, Richard M., "Sources and Sinks of Radiative Energy From 30 to 90 km," *Quarterly Journal of the Royal Meteorological Society*, Vol. 84, No. 361, London, England, July **1958**, pp. 225–234.

Nakayama, Toshio, Kitamura, Morris Y., and Matanabe, K., "Ionization Potential and Absorption Coefficients of Nitrogen Dioxide," *Journal of Chemical Physics*, Vol. 30, No. 5, May **1959**, pp. 1180–1186.

Nicolet, M., "Ozone and Hydrogen Reactions," *Annales de Geophysique*, Vol. 26, No. 2, Lille, France, April–June **1970**, pp. 531–546.

Ogura, Yoshimitsu, and Phillips, Norman A., "Scale Analysis of Deep and Shallow Convection in the Atmosphere," *Journal of the Atmospheric Sciences*, Vol. 19, No. 2, Mar. **1962**, pp. 173–179.

Paraskevopoulos, G., and Cvetanovic, R. J., "Relative Rate of Reaction of $O(^1D)$ With H_2O" *Chemical Physics Letters*, Vol. 9, No. 6, June 15, **1971**, pp. 603–605.

Paukert, Thomas T., and Johnston, Harold S., "Spectra and Kinetics of the Hydroperoxyl Free Radical in the Gas Phase," *Journal of Chemical Physics*, Vol. 56, No. 6, Mar. 15, **1972**, pp. 2824–2838.

Pearce, Jeffery B., "Rocket Measurement of Nitric Oxide Between 60 and 96 Kilometers," *Journal of Geophysical Research, Space Physics*, Vol. 74, No. 3, Mar. 1, **1969**, pp. 853–861.

Phillips, L. F., and Schiff, H. I., "Mass Spectrometric Studies of Atomic Reactions. III. Reactions of Hydrogen With Nitrogen Dioxide and With Ozone," *Journal of Chemical Physics*, Vol. 37, No. 6, Sept. **1962**, pp. 1233–1238.

Rawcliff, R. D., Meloy, G. E, Friedman, R. M., and Rogers, E. H., "Measurement of Vertical Distribution of Ozone From a Polar Orbiting Satellite," *Journal of Geophysical Research*, Vol. 68, No. 24, Dec. 15, **1963**, pp. 6425–6429.

Rodgers, C. D., and Walshaw, C. D., "The Computation of Infrared Cooling in Planetary Atmospheres," *Quarterly Journal of the Royal Meteorological Society*, Vol. 92, No. 391, London, England, Jan. **1966**, pp. 67–92.

Schiff, H. I., "Neutral Reactions Involving Oxygen and Nitrogen," *Candian Journal of Chemistry*, Vol. 47, No. 10, Ottawa, Canada, May 15, **1969**, pp. 1903–1916.

Schmidt, S. C., Amme, R. C., Murcray, D. G., and Goldman, A., "Ultraviolet Absorption by Nitric Acid Vapour," *Nature, Physical Science*, Vol. 238, London, England, Aug. **14, 1972**, p. 109.

Schofield, K., "An Evaluation of Kinetic Rate Data for Reactions of Neutrals of Atmospheric Interest," *Planetary and Space Science*, Vol. 15, No. 4, Oxford, England, Apr. **1967**, pp. 643–670.

Schölz, T. G., Ehhalt, D. H., Heidt, L. E., and Martell, E. A., "Water Vapor, Molecular Hydrogen, Methane, and Tritium Concentrations Near the Stratopause," *Journal of Geophysical Research*, Vol. 75, No. 15, May 20, **1970**, pp. 3049–3054.

Schütz, K., Junge, C., Beck, R., and Albrecht, B., "Studies of Atmospheric N_2O," *Journal of Geophysical Research*, Vol. 75, No. 12, Apr. 20, **1970**, pp. 2230–2245.

Shimazaki, Tatsuo, and Laird, A. R., "A Model Calculation of the Diurnal Variation in Minor Neutral Constituents in the Mesosphere and Lower Thermosphere Including Transport Effects," *Journal of Geophysical Research, Space Physics*, Vol. 75, No. 16, June 1, **1970**, pp. 3221–3235.

Theon, J. S., and Smith, W. S., "The Meteorological Structure of the Mesosphere Including Seasonal and Latitudinal Variations," Mesospheric Models and Related Experiments, *Proceedings of the Fourth Esrin-Eslab Symposium, Frascati, Italy, July 6–10*, **1970**, Astrophysics and Space Science Library, D. Reidel Publishing Company, Dordrecht, Holland, **1971**, pp. 131–146.

Thompson, B. A., Harteck, P., and Reeves, R. R., Jr., "Ultraviolet Absorption Coefficients of CO_2, CO, O_2, H_2O, NH_3, NO, SO_2, and CH_4 between 1850 and 4000Å," *Journal of Geophysical Research*, Vol. 68, No. 24, Dec. 15, **1963**, pp. 6431–6436.

Valley, Shea L. (Editor), *Handbook of Geophysics and Space Environments*, McGraw-Hill Book Co., New York, N.Y., **1965** (see "Tropical Supplemental Atmospıere," p. 2–11).

Van Allen, J. A. and Hopfield, J. J., "Preliminary Report on Atmospheric Ozone Measurements from Rockets", *Societé Royale des Sciences de Liege–Memoires*, Vol. 12, Belgium, **1952**, pp. 179–183.

Watanabe, K., and Zelikoff, Murray, "Absorption Coefficients of Water Vapor in the Vacuum Ultraviolet," *Journal of the Optical Society of America*, Vol. 43, No. 9, Sept. **1953**, pp. 753–755.

Weeks, L. H., and Smith, L. G., "A Rocket Measurement of Ozone Near Sunrise," *Planetary and Space Science*, Vol. 16, No. 9. Oxford, England, Sept. **1968**, pp. 1189–1195.

Zipf, E. C., "The Collisional Deactivation of Metastable Atoms and Molecules in the Upper Atmosphere," *Canadian Journal of Chemistry*, Vol. 47, No. 10, Ottawa, Canada, May 15, **1969**, pp. 1863–1877.

[*Received November 24, 1972; revised May 14, 1973*]